

## ABSTRACT

LEWIS, JOHN DONAVER. Assessment of a Single-ring Sprinkle Infiltrometer Method for Evaluating Soil-based Stormwater Management Practices. (Under the direction of Dr. Joshua L. Heitman).

Rapid urbanization in the Southeastern U.S. is expected to have broad environmental impacts. One challenge in diminishing these impacts is managing increased stormwater runoff caused by greater impervious surface. Soil-based stormwater mitigation strategies often involve alteration of disturbed soils, resulting in soil layering with highly conductive soil layers overlying less permeable layers. Measurements used to evaluate infiltration into these modified soils may not accurately represent stormwater flow. In particular, single-ring sprinkle infiltrometer methods (e.g., the Cornell Sprinkle Infiltrometer) are being used with increasing frequency to assess stormwater management practices, but their limitations have not been thoroughly tested. Single-ring infiltrometers are subject to lateral flow beneath the ring, potentially causing observed infiltration rate ( $i_s$ ) to exceed the vertical infiltration rate ( $i_v$ ) measurements are intended to represent. The primary objective of this study was to assess the Cornell Sprinkle Infiltrometer (CSI) method for evaluating infiltration into layered soils. Two approaches were taken: the CSI infiltrometer was compared with a commonly-used ponded, double-ring infiltrometer using field measurements; and numerical simulations were used to assess CSI performance over a range of layered soil conditions in comparison to vertical flow. The  $i_s$  from CSI and ASTM standard double-ring (DRI) methods was compared for 13 conditions. Overall, the CSI method gave 2% greater  $i_s$ . Regression of  $i_s$  with subsurface layer saturated hydraulic conductivity ( $K_s$ ) showed strong correlation for both methods ( $R^2 = 0.87$  and  $R^2 = 0.83$  for CSI and DRI methods, respectively). Numerical simulations, performed using HYRDUS 2D, were used to test the effects of depth to subsurface layer ( $L$ ) and contrast between

surface and subsurface layer  $K_S$  on CSI  $i_S$  relative to  $i_v$  ( $i_S/i_v$ ). Effects from  $L$  were dependent on contrast in layer  $K_S$ . The  $i_S/i_v$  approached 1 (i.e., infiltrometers provided results similar to vertical infiltration) when layer  $K_S$  was within one order of magnitude. Layer  $K_S$  contrasts greater than an order of magnitude gave large  $i_S/i_v$ , indicating that the CSI over-estimated infiltration. Overall, the CSI approach gave results similar to other tested measurement methods, and simulated measurements matched  $i_v$  when the difference between layer hydraulic properties was not extreme. Understanding the relationship between ring infiltrometer measurements and natural infiltration processes will provide more effective evaluations of soil management practices that create layered conditions.

© Copyright 2016 John Donaver Lewis

All Rights Reserved

Assessment of a Single-ring Sprinkle Infiltrometer Method for Evaluating Soil-based Stormwater  
Management Practices

by  
John Donaver Lewis

A thesis submitted to the Graduate Faculty of  
North Carolina State University  
in partial fulfillment of the  
requirements for the Degree of  
Master of Science

Soil Science

Raleigh, North Carolina

2016

APPROVED BY:

---

Michael Burchell

---

Richard McLaughlin

---

Joshua Heitman  
Chair of Advisory Committee

## **BIOGRAPHY**

John Lewis is originally from Wilmington, North Carolina. He holds bachelor's degrees in Geology from UNCW and Natural Resources from NC State. John hopes to dedicate his professional career to making positive impacts on issues involving land and water resources.

## TABLE OF CONTENTS

LIST OF TABLES .....	iv
LIST OF FIGURES .....	v
Chapter 1: Introduction and Background Information.....	1
References.....	4
Figure .....	7
Chapter 2: Comparison of Single- and Double-ring Methods of Measuring Steady Infiltration Rate in Layered Soils .....	8
Abstract.....	8
Introduction.....	9
Materials and Methods.....	12
Field Sites.....	12
Infiltration Measurements.....	13
Soil Property Measurements .....	14
Analyses.....	14
Results and Discussion .....	15
Soil Materials .....	15
Infiltration Measurement Method Comparison .....	15
Layer $K_S$ Comparison .....	17
Comparison of $i_s$ with Subsurface $K_S$ .....	18
Conclusion .....	18
References.....	19
Tables.....	23
Figures.....	27
Chapter 3: Numerical Assessment of a Single-ring Sprinkle Infiltrometer Method for Measuring Steady Infiltration Rate of Layered Soils.....	31
Abstract .....	31
Introduction.....	32
Materials and Methods.....	33
Infiltration Measurements.....	33
Soil Property Measurements .....	34
Numerical Simulations and Validation.....	34
Analyses .....	36
Results and Discussion .....	37
Depth Effect on Infiltrometer Measurement.....	37
Contrasting Layer $K_S$ Effect on Infiltrometer Measurement .....	38
Conclusion .....	39
References.....	40
Tables.....	43
Figures.....	45
Chapter 4: Conclusions and Future Work.....	51
Conclusions.....	51
Future Work .....	52

## LIST OF TABLES

<b>Table 2.1.</b> Soil texture for layered materials at four sites. ....	23
<b>Table 2.2.</b> Site management practices and bulk density by depth for surface and subsurface materials. ....	24
<b>Table 2.3.</b> Comparison of steady infiltration rate ( $i_s$ ) values measured using single- and double-ring infiltrometer. ....	25
<b>Table 2.4.</b> Saturated hydraulic conductivity ( $K_s$ ) values for surface and subsurface materials. ....	26
<b>Table 3.1.</b> Soil material properties and inputs for two case studies. ....	43
<b>Table 3.2.</b> Selected input parameters and domain information for numerical simulations. ....	44

## LIST OF FIGURES

**Figure 1.1.** Illustrations showing infiltration from rainfall into uniform (a) and layered (b) soils and infiltration from single-ring infiltrometers into uniform (c) and layered (d) soils next to plots of saturated hydraulic conductivity ( $K_S$ ) with depth..... 7

**Figure 2.1.** Linear regression of double-ring  $i_S$  versus single-ring  $i_S$  for layered conditions. Points are geometric means of  $i_S$  for each set of conditions. Error bars are one standard deviation from the mean. ....27

**Figure 2.2.** Linear regression of double-ring  $i_S$  versus single-ring  $i_S$  with texture-based correction applied for single-ring measurements. Points are geometric means of  $i_S$  for each set of conditions. Error bars are one standard deviation from the mean. ....28

**Figure 2.3.** Linear regressions of steady infiltration rate ( $i_S$ ) with single- and double-ring infiltrometers versus saturated hydraulic conductivity ( $K_S$ ) for subsurface layers.....29

**Figure 2.4.** Axisymmetric schematics of experimental conditions from single-ring infiltrometer measurements in layered soil. Depths to subsurface layer ( $L$ ) equal to 15 cm (a) and 30 cm (b). Ring depth ( $d$ ) = 15 cm. Dotted line represents layer boundary.....30

**Figure 3.1.** HYDRUS 2D domain geometry and boundary condition information for ring infiltrometer simulations.....45

**Figure 3.2.** Simulation validation curves for Case 1 (a) and Case 2 (b) infiltrometer measurements.....46

**Figure 3.3.** Example vertical infiltration rate ( $i_v$ ) water content distribution (a) with infiltration rate curve (b) and example single-ring steady infiltration rate ( $i_S$ ) water content distribution (c) with infiltration rate curve (d) for 60 min. simulation using Case 1 conditions. ....47

**Figure 3.4.** Numerical simulation results showing effect of layer depth ( $L$ ) on steady infiltration rate ( $i_S$ ) from single-ring, sprinkle infiltrometer method. ....48

**Figure 3.5.** Numerical simulation results showing effect of layer  $K_S$  on steady infiltration measured from single-ring sprinkle infiltrometer ( $i_S$ ) for Case 1. ....49

**Figure 3.6.** Numerical simulation results showing effect of layer  $K_S$  on steady infiltration rate measured from single-ring sprinkle infiltrometer ( $i_S$ ) for Case 2. ....50



## **Chapter 1: Introduction and Background Information**

Urban land area in the Southeastern U.S. is expected to increase 139% by 2060 as forested, agricultural and pasture land decreases (Terando et al., 2014). This change in land use will likely alter hydrologic regimes within the region, decreasing infiltration of stormwater and increasing stormwater runoff. Much of this increased runoff will be caused by increased impervious surface (Boggs and Sun, 2011), though the remaining exposed soil becomes disturbed through the development process (Pitt et al., 1999). Often, unintended impacts of construction practices (e.g., clearing and grading) lead to a reduced ability for soil to infiltrate water (Gregory et al., 2006; Pitt et al., 2008; Woltemade, 2010). These impacts must be mitigated in order to prevent potential degradation of water resources. Low Impact Development (LID) is a strategy that may be implemented. The goal of LID is to preserve pre-development hydrologic conditions within a watershed (Prince George's County, 1999). Soil-based LID strategies that promote infiltration before it becomes runoff involve disruption or alteration of the disturbed surface, usually through tillage or addition of some amendment (Haynes et al., 2013; Pitt et al., 1999; Olson et al., 2013). These practices result in a layered soil condition where more hydraulically conductive surface layer overlays and less hydraulically a surface layer with relatively high infiltration capacity overlays a lower infiltration capacity subsurface layer (Figure 1.1).

To determine the efficacy of these management practices, infiltration measurements are often used. There are three common field techniques for measuring infiltration: ring infiltrometers, which are typically implemented with ponded-head conditions; rainfall simulators, which apply water at a known rate over a large surface area (relative to ring infiltrometers) and are useful for determining time to runoff; and tension infiltrometers which are

designed to measure flow in the soil matrix (Youngs, 1991). Ring infiltrometer measurements have been thoroughly examined in scientific literature. The ponded condition used with ring infiltrometers allows for determination of flow approaching the steady-state condition (Reynolds et al., 2002a). This steady flow from a ring infiltrometer is often related to the effective saturated hydraulic conductivity at the surface (Reynolds et al., 2002b). Flow beneath the ring, however, is subject to lateral movement, potentially leading to overestimation of infiltration in the vertical direction (Reynolds and Elrick, 1990). Double-ring infiltrometer methods employ buffer rings to limit lateral flow (Burgy and Luthin, 1956; Swartzendruber and Olson, 1961). Constant-head ring infiltrometers methods are often cumbersome and require transport of large amounts of water to the measurement area as well as long time periods to reach steady rates (Ahuja et al., 1976; Gregory et al., 2005; Maheshwari, 1996).

Rainfall simulators allow for measurement conditions that represent infiltration and runoff processes, though ring infiltrometer methods allow for determination of soil hydrological properties (Touma and Albergel, 1992). The Cornell Sprinkle Infiltrometer (CSI) method combines the more representative boundary condition of a rainfall simulator with the robust application of a ring infiltrometer (Ogden et al., 1997). This method may provide more effective evaluations of the previously described LID practices. In addition, the CSI method is mostly self-contained and more easily transported compared to other types of infiltrometers (van Es and Schindelbeck, 2003).

The primary goal of this research is to assess the CSI method for the purpose of evaluating management practices specifically designed to improve stormwater infiltration. A result of the analysis conducted for this research was the emergence of two secondary goals; to determine the effect of soil layering on CSI measurements (Fig. 1.1c and Fig. 1.1d) and to relate

these measurements to one-dimensional vertical infiltration analogous to rainfall events (Fig 1.1a and Fig. 1.1b). In Chapter 2, a comparison between the CSI method and a more commonly-used ASTM standard double-ring method (ASTM, 2009) is presented. In Chapter 3, results from numerical simulations of the CSI method performed using HYDRUS 2D (Simunek et al., 2006) are discussed for layered soil conditions. A summary of this research is presented in Chapter 4 along with suggestions for further research on these subjects.

## REFERENCES

- Ahuja, L.R., El-Swaify, S.A., Rahman, A., 1976. Measuring hydrologic properties of soil with a double-ring infiltrometer and multiple-depth tensiometers. *Soil Science Society of America Journal* 40, 494–499.
- ASTM, 2009. Standard test method for infiltration rate of soils in field using double-ring infiltrometer. ASTM International 10.
- Boggs, J.L., Sun, G., 2011. Urbanization alters watershed hydrology in the Piedmont of North Carolina. *Ecohydrology* 4, 256–264.
- Burgy, R.H., Luthin, J.N., 1956. A test of the single-and double-ring types of infiltrometers. *Eos, Transactions American Geophysical Union* 37, 189–192.
- Gregory, J.H., Dukes, M.D., Jones, P.H., Miller, G.L., 2006. Effect of urban soil compaction on infiltration rate. *Journal of Soil and Water Conservation* 61, 117–124.
- Gregory, J.H., Dukes, M.D., Miller, G.L., Jones, P.H., 2005. Analysis of Double-Ring Infiltration Techniques and Development of a Simple Automatic Water Delivery System. *ats* 2, 0. doi:10.1094/ATS-2005-0531-01-MG
- Haynes, M.A., McLaughlin, R.A., Heitman, J.L., 2013. Comparison of methods to remediate compacted soils for infiltration and vegetative establishment. *Open Journal of Soil Science* 3, 225.
- Maheshwari, B.L., 1996. Development of an automated double-ring infiltrometer. *Soil Research* 34, 709–714.
- Ogden, C.B., Van Es, H.M., Schindelbeck, R.R., 1997. Miniature rain simulator for field measurement of soil infiltration. *Soil Science Society of America Journal* 61, 1041–1043.

- Olson, N.C., Gulliver, J.S., Nieber, J.L., Kayhanian, M., 2013. Remediation to improve infiltration into compact soils. *Journal of Environmental Management* 117, 85–95.  
doi:10.1016/j.jenvman.2012.10.057
- Pitt, R., Chen, S.-E., Clark, S.E., Swenson, J., Ong, C.K., 2008. Compaction's Impacts on Urban Storm-Water Infiltration. *Journal of Irrigation and Drainage Engineering* 134, 652–658.  
doi:10.1061/(ASCE)0733-9437(2008)134:5(652)
- Pitt, R., Lantrip, J., Harrison, R., Henry, C., and Hue, D., 1999. "Infiltration through disturbed urban soils and compost-amended soil effects on runoff quality and quantity." EPA 600/R-00/016, U.S. Environmental Protection Agency, Water Supply and Water Resources Division, National Risk Management Research Laboratory, Cincinnati.
- Prince George's County, 1999. Low-impact development design strategies: An integrated design approach. Department of Environmental Resources, Programs and Planning Division, Prince George's County, Maryland.
- Reynolds, W.D., Elrick, D.E., 1990. Poned infiltration from a single ring: I. Analysis of steady flow. *Soil Science Society of America Journal* 54, 1233–1241.
- Reynolds, W.D., Elrick, D.E., Youngs, E.G., 2002a. Ring or cylinder infiltrometers (vadose zone). *Methods of soil analysis. Part 4*, 818–826.
- Reynolds, W.D., Elrick, D.E., Youngs, E.G., 2002b. Single-ring and double-or concentric-ring infiltrometers. *Methods of soil analysis. Part 4*, 821–826.
- Simunek, J., Van Genuchten, M.T., Sejna, M., 2006. The HYDRUS software package for simulating two and three-dimensional movement of water, heat, and multiple solutes in variably-saturated media. Technical manual 1.

- Swartzendruber, D., Olson, T.C., 1961. Sand-model study of buffer effects in the double-ring infiltrometer. *Soil Science Society of America Journal* 25, 5–8.
- Terando, A.J., Costanza, J., Belyea, C., Dunn, R.R., McKerrow, A., Collazo, J.A., 2014. The southern megalopolis: using the past to predict the future of urban sprawl in the Southeast US. *PloS one* 9, e102261.
- Touma, J., Albergel, J., 1992. Determining soil hydrologic properties from rain simulator or double ring infiltrometer experiments: a comparison. *Journal of hydrology* 135, 73–86.
- Woltemade, C.J., 2010. Impact of residential soil disturbance on infiltration rate and stormwater runoff. *Wiley Online Library*.
- Youngs, E.G., 1991. Infiltration measurements—a review. *Hydrological processes* 5, 309–319.
- van Es, H.M., Schindelbeck, R.R., 2003. Field procedures and data analysis for the Cornell sprinkle infiltrometer. Department of Crop and Soil Science Research Series R03-01. [soilhealth.cals.cornell.edu](http://soilhealth.cals.cornell.edu).

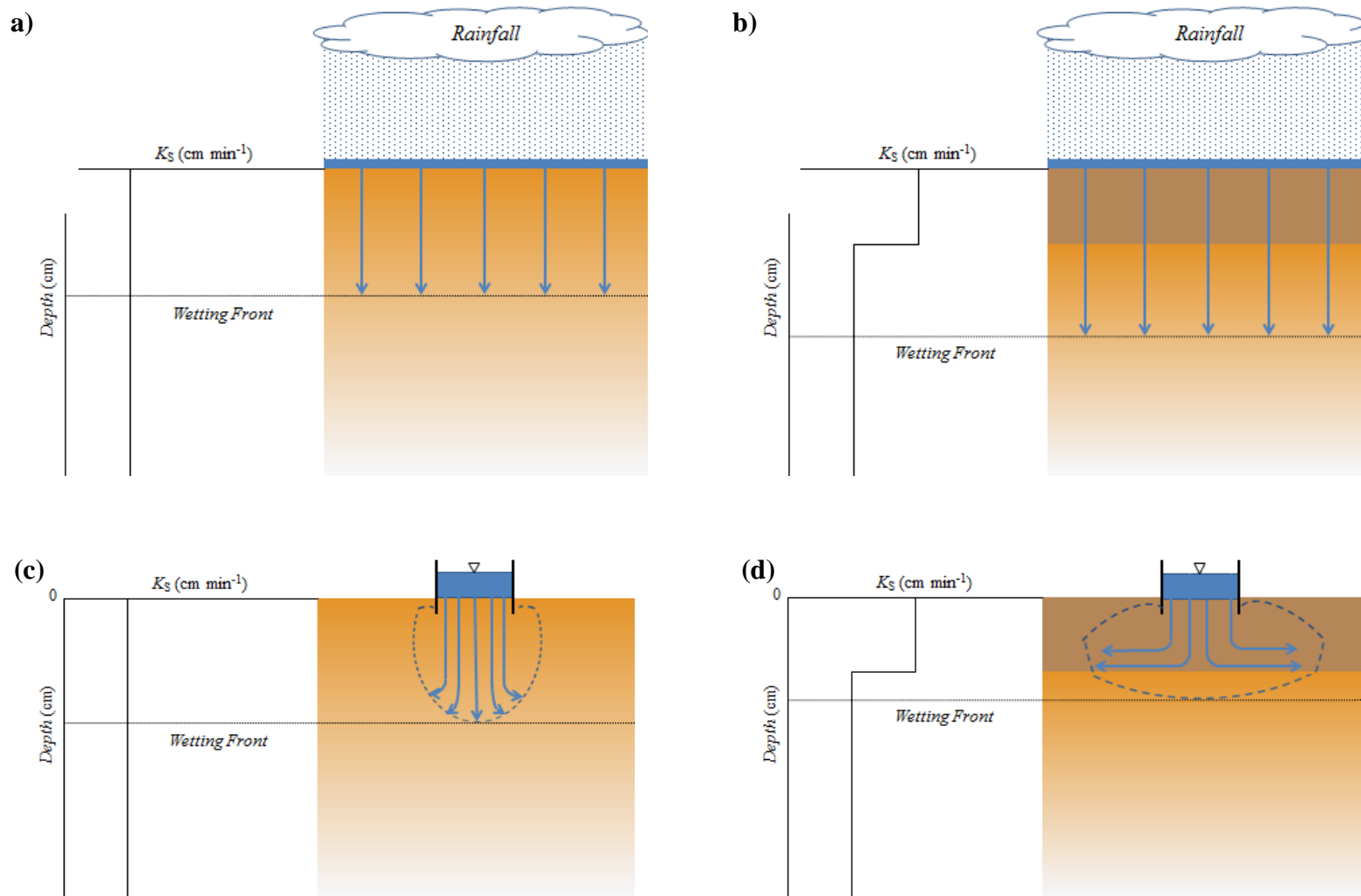


**Figure 1.1.** Illustrations showing infiltration from rainfall into uniform (a) and layered (b) soils and infiltration from ring infiltrometers into uniform (c) and layered (d) soils next to plots of saturated hydraulic conductivity ( $K_S$ ) with depth.

## Chapter 2: Comparison of Single- and Double-ring Methods of Measuring Steady Infiltration Rate in Layered Soils

### ABSTRACT

Infiltration rate measurements are used to evaluate land management practices designed to improve infiltration. While consistent methodologies used for differing sites and/or conditions can be compared directly, comparison across methodologies is difficult. Relating field infiltration rate measurements to the natural infiltration process is also challenging due to constraints on boundary conditions and flow imposed in applying measurement methodologies. Practices such as tillage create conditions where a more permeable layer overlays an impeding layer. This further complicates comparison of infiltration measurements to natural infiltration processes. The primary objective of this study was to compare two ring infiltrometer methods for measuring steady infiltration rate ( $i_s$ ) on layered soils: the Cornell Sprinkle Infiltrometer (CSI) method; and the ASTM double-ring (DRI) method. Measurements were made at four sites in Wake County, NC. Four replications of thirteen sets of conditions (52 total paired measurements) were made. Conditions were defined by site and management practice. Soil texture, bulk density, and saturated hydraulic conductivity ( $K_s$ ) were measured at the soil surface and in the subsurface to assess soil layering within sets of conditions. A regression was used to compare selected conditions for both methods had a linear relationship ( $R^2 = 0.79$ ). The difference between methods was minimal (3% greater overall for CSI  $i_s$  compared to DRI measurements). A linear regression was used to compare subsurface  $K_s$  to CSI  $i_s$  ( $R^2 = 0.87$ ) and DRI  $i_s$  ( $R^2 = 0.83$ ). Measurements were grouped by subsurface layer depth, indicating that  $i_s$  may be related to subsurface  $K_s$  depending on depth to this layer.



## INTRODUCTION

Soil infiltration rate is a property commonly used in evaluating sites where understanding water movement into soil is critical. Soil infiltration rate measurements have been used to: assess strategies for managing soil for urban stormwater runoff (Emerson and Traver, 2008; Haynes et al., 2013), monitor the improvement of land restoration practices (Liu et al., 2012; Perkins et al., 2014), and determine impacts of agricultural activities on soil properties (Franzluebbers et al., 2012; Oliveira and Merwin, 2001), among many others. Many of these practices involve alteration of the upper portion of a disturbed soil profile by using tillage and establishing vegetation to encourage the development of soil structure. These practices commonly create layering where a less dense, more hydraulically conductive material overlays a more dense, less hydraulically conductive material.

Ring infiltrometers are commonly used for measuring soil infiltration rate. Many interpretations of ring infiltrometer measurements have been used to characterize soils. Single-ring infiltrometers are subject to lateral movement of water beneath the ring where matric flux dominates flow at the wetting front (Reynolds and Elrick, 1990). DRI methods are often used to reduce the influence of matric potential by creating a “buffer zone” around the measurement ring (Reynolds et al., 2002). Previous comparisons of single- and double-ring methods have shown mixed results, depending on the measurement conditions and the approach used. Burgy and Luthin (1956) showed that there was no statistical difference between single- and double-ring infiltrometers using a falling head method on a homogeneous Yolo silt loam. Swartzendruber and Olson (1961) showed using buffer rings gave results more similar to true vertical infiltration rate for a homogeneous sand, the degree to which was dependent on measurement time and ring geometry. Ahuja et al. (1976) reported the extent of lateral flow using tensiometers and that

steady infiltration rate took longer to achieve when no buffer ring was used. Youngs (1987) showed that the effectiveness of buffer rings depends on ring diameter and depth of insertion. Wu et al. (1997) used numerical simulations to determine ratio of lateral flow to vertical flow for both single- and double-ring infiltrometers in three different soil materials. The double-ring infiltrometers resulted in lower infiltration rate values than the single-ring infiltrometers, though the double-ring values were far from the true vertical infiltration rate (depending on buffer ring diameter). Wu et al. (1997) also found that simulated infiltration in layered soils depended on the depth of the layering and time of measurement. Verbist et al. (2010) showed that single- and double-ring infiltrometers were not statistically different for numerous calculation methods on stony soils.

Ring infiltrometer measurements constitute infiltration from a point source. Bouwer (1986) and Hillel (1998) describe a perching effect when they are used in the layered soils mentioned above. The relationship of steady infiltration rate measured using ring infiltrometers ( $i_s$ ) to one dimensional, vertical steady infiltration rate ( $i_v$ ) in layered soil profiles is difficult to determine. For a homogeneous soil,  $i_v$  is approximately equal to the saturated hydraulic conductivity ( $K_S$ ) in the vertical direction (Hillel, 1998). At large times,  $i_s$  approaches  $K_S$  asymptotically (Reynolds et al., 2002). This relationship may be summarized by:

$$i_v \approx K_S \approx i_s$$

In layered soils,  $i_v$  at large times is controlled by  $K_S$  of the most hydraulically limiting layer. The  $i_s$  becomes exaggerated relative to  $i_v$  due to increased lateral flow caused by the perching effect. The relationship of  $i_v$ ,  $K_S$ , and  $i_s$  in layered soils with greater hydraulic conductivity in the surface layer, compared to the subsurface, may be expressed by:

$$i_v \approx K_{\text{eff}} \leq i_s$$

where  $K_{\text{eff}}$  represents effective  $K_S$  as affected by subsurface properties.

Comparison of  $i_S$  using a consistent methodology provides sound scientific basis for assessing soil infiltration rate for land management purposes. Comparison of management conditions using inconsistent methodologies may lead to variation in interpretations of results (Reynolds et al., 2000; Verbist et al., 2010). Double-ring infiltrometer methods have been used since the 19<sup>th</sup> century (Daniel, 1952). Standard ponded double-ring infiltrometer tests can be cumbersome to use in the field because of the large supply of water required and the amount of time to set up the apparatus and subsequently reach  $i_S$  (Elrick et al., 2002; Maheshwari, 1996). Additionally, ponded infiltration may not adequately represent conditions in which rainfall is partitioned into both infiltration and runoff on surfaces that don't confine or pond water. Rainfall simulators allow for more realistic representations of natural infiltration and runoff processes where surface water is not confined, though they may underestimate  $i_S$  as a result of surface sealing from raindrop impacts (Touma and Albergel, 1992). The Cornell Sprinkle Infiltrometer (CSI) is a mostly self-contained apparatus that allows the effects from ponded infiltration to be neglected, i.e. unsaturated infiltration can be recorded in addition to  $i_S$  with minimal disturbance (Ogden et al., 1997). For these reasons, the CSI may provide advantages over ponded infiltration methods. The single-ring component of the CSI, however, may result in exaggerated lateral flow in layered soils compared to double-ring infiltrometer methods which are designed to limit lateral flow. The  $i_S$  measured using the CSI may therefore be greater than  $i_S$  measured using double ring infiltrometers. The primary objective of this study is to compare two ring infiltrometer methods, the CSI method and the ASTM standard double-ring (DRI) method (2009), for interpretation of  $i_S$  into layered soils. An effort was made to relate  $i_S$  to  $i_v$  to determine whether ring infiltrometer measurements could be related to infiltration from rainfall

events. It was hypothesized that layer depth, ring geometry, and subsurface  $K_S$  would be factors in a one-dimensional, mathematical model relating  $i_S$  to  $i_v$ .

## **MATERIALS AND METHODS**

### **Field Sites**

CSI and DRI measurements were made at four locations in Wake County, NC to capture  $i_S$  over a range of soil conditions with differing management practices. Three of the sites were located at NC State University facilities including; the Sediment and Erosion Control Research and Extension Facility (SECREF), the Central Crops Research Station (CCRS), and the Lonnie Poole Golf Course (LP). The fourth site was an Interstate 40-Eastbound off-ramp at Jones Sausage Rd. in Garner, NC (JS).

SECREF, LP, and JS were plot-scale study sites at which tillage and vegetation establishment were being tested to improve stormwater infiltration into compacted soils. Plot sizes at SECREF were  $5.0 \times 2.5$  m and were  $2.5 \times 1.5$  m at both JS and LP. CCRS fields were not being used for crop production at the time of measurement. SECREF plots consisted of fill material from a local construction project, spread on exposed subsoil, and compacted. Tillage (T) was the primary management practice at all sites. JS and LP were tilled to a maximum depth of 15 cm, and SECREF and CCRS were tilled to a maximum depth of 30 cm. Additionally, a subset of plots at each site also had amendments: compost was incorporated (TC) at SECREF, JS, and LP; and amendments including polyacrylamide (TP) and gypsum (TG) were incorporated at SECREF. Measurements were made on one fallow (F) hayfield at CCRS. Control (N) conditions included no tillage practice in the time preceding field measurements. Physical properties are summarized in Tables 2.1 and 2.2. In all, measurements were collected

for four replications of 13 conditions across four sites, totaling 52 paired CSI and DRI measurements.

### **Infiltration Measurements**

CSI measurements were made using the method outlined in its manual (van Es and Schindelbeck, 2003). The CSI consists of a miniature rainfall simulator combined with a single ring. The ring has a hole in its exterior that prevents water from ponding. “Runoff” from within the ring is collected through a tube affixed to the hole. Infiltration is measured by taking the difference between the volume of water applied by the rainfall simulator and the volume of runoff exiting the ring per unit time. Ring diameter was 24.1 cm and ring insertion depth was 15 cm. Rainfall rate was between 30 and 60 cm h<sup>-1</sup> in order to ensure that runoff was generated and multiple measurements could be made. Rainfall and runoff were recorded at one-minute intervals. CSI measurements were 0.3 to 1.5 hours in duration, depending on the time required to achieve a constant infiltration rate. The  $i_s$  was considered reached when ten consecutive runoff volumes were within 1.3 cm h<sup>-1</sup> of one another.

DRI  $i_s$  was measured according to the method outlined in the ASTM standard (ASTM, 2009). The DRI apparatus consisted of two concentric rings, separate water supplies for inner and outer rings, and float valves for maintaining constant height of ponding within the rings. Inner and outer ring diameters were 25.0 and 50.0 cm respectively. Ring insertion depth was 7.5 cm for the inner ring and 10.0 cm for the outer ring. Height of ponding ranged from 5.0 to 10.0 cm above the soil surface. The  $i_s$  was reached once a constant height of ponding was established in both the inner and outer ring. Once established,  $i_s$  was measured by recording the water level in the inner ring water supply over intervals of 0.08 to 0.5 hours. Measurements were made at various time intervals for 0.5 to 3.0 hours once  $i_s$  was reached.

## Soil Property Measurements

Manipulation of pre-existing soil conditions using management practices was hypothesized to result in soil layers with distinct properties. Using this assumption, the “surface” layer was considered as the manipulated soil material and the “subsurface” layer was considered to be the material underlying the maximum depth of tillage. Soil particle size distribution, bulk density, and  $K_S$  were measured using core samples (7.5 cm in diameter and 7.5 cm in height) extracted from within each layer. Samples were extracted from the surface to 7.5 cm depth at each measurement position and below the maximum depth of tillage for all sites, with additional sampling depths of 7.5 to 15.0 cm and 15.0 to 22.5 cm for SECREF. Subsurface samples were collected within the measurement area for SECREF and CCRS sites and outside of the plot area for JS and LP. Individual samples were collected for each plot or measurement position for SECREF and CCRS, but were not collected individually within each plot for JS and LP. This was to minimize disturbance of an ongoing study at JS and LP. Particle size distribution was measured using the hydrometer method (Day, 1965) and bulk density was measured using the core method (Blake, 1965). A constant-head, benchtop method was used to measure  $K_S$  (Klute and Dirksen, 1986) with the following calculation:

$$K_S = \frac{V}{At} \left( \frac{L}{H} \right),$$

where  $V$  ( $m^3$ ) is volume measured as discharge from soil cores (outflow),  $A$  ( $m^2$ ) is area of soil core,  $t$  is time (min),  $L$  (m) is length of soil within core, and  $H$  (m) is the hydraulic head ( $L +$  height of ponding). Heights of ponding within soil cores were maintained at 4 to 6 cm.

## Analyses

Statistical analyses were performed to compare measurement conditions by soil properties and measurement methods by  $i_s$  values. Hydraulic conductivity measurements

frequently exhibit log-normal distribution (Bagarello and Provenzano, 1996; Freeze, 1975; Lee et al., 1985; Wilson and Luxmoore, 1988). Arithmetic mean ( $i_{AR}$ ), geometric mean ( $i_{GM}$ ), and coefficients of variation (CV) were calculated for CSI and DRI  $i_S$  by condition. Likewise, arithmetic mean ( $K_{AR}$ ), geometric mean ( $K_{GM}$ ) and CV were calculated for surface and subsurface  $K_S$  by condition. CSI and DRI  $i_S$  was compared using analysis of variance (ANOVA) and linear regression. ANOVA was performed to test differences between surface  $K_S$  and subsurface  $K_S$ . The CV was calculated and ANOVA was performed for  $i_S$  and  $K_S$  using  $i_{AR}$  and  $K_{AR}$ , respectively. CSI and DRI  $i_S$  were related to one other by  $i_{AR}$  in a linear regression, and  $K_S$  was related to  $i_S$  using the respective geometric means in a linear regression.

## **RESULTS AND DISCUSSION**

### **Soil Materials**

Soil textures ranged from sand to clay loam (Table 2.1). Only the CCRS “F” field and JS had uniform textural classes throughout the depth of measurement. SECREf fill material was sandy clay loam overlaying clay loam subsoil. The CCRS “T” field was sand overlaying loamy sand. LP was sandy clay loam overlaying clay loam. Bulk densities ranged from 1.16 to 1.83 g cm<sup>-3</sup> across all conditions (Table 2.2). Results from the physical property measurements indicate a wide range of conditions between and within sites.

### **Infiltration Measurement Method Comparison**

The two methods had different degrees of variability in  $i_S$  for each set of conditions (Table 2.3). Variability for CSI  $i_S$  measurements was minimal (CV < 10.0%) for all conditions except for LP TC (12.4%) and LP N conditions (106%). Four conditions showed substantial variability (CV > 64.0%) for DRI measurement  $i_S$ , including SECREf N, JS T, JS N, and LP N. Among these, JS N and SECREf TC conditions had significant difference between methods at  $p$

= 0.05. Runoff was not observed on three out of four SECREf TC plots indicating  $i_s$  was not reached. The lowest average  $i_s$  values were measured at sites with 15 cm tillage (JS and LP). These conditions also had the greatest variability (CV > 10.0%) in DRI  $i_s$  (Table 2.3).

CSI and DRI  $i_s$  values were compared using a linear regression (Fig. 2.1). Only conditions showing limited variability were considered in the regression (JS T and all N conditions were removed). SECREf TC conditions were also not considered, as  $i_s$  was not reached for three out of four plots. The regression equation was  $y = 1.03x$ , indicating that the CSI  $i_s$  was 3% greater overall compared to DRI  $i_s$  for the selected conditions (Fig. 2.1). The correction factors suggested by van Es and Schindelbeck (2003), intended to correct for lateral movement once flow moves beneath the ring, did not improve the correlation between the methods ( $R^2 = 0.79$  for non-corrected and corrected CSI values), but did reduce the difference between  $i_s$  from 3% to 2% (Fig. 2.2). Under these layered soil conditions, it is possible that improvements based on the proposed correction factors were less significant than the effect of layering.

The CSI has been compared with double-ring methods by Zwirtes et al. (2013) and Barrett and Rodgers (2015). Zwirtes et al. (2013) reported greater  $i_s$  values using the DRI method compared to the CSI method for three different management practices in a Rhodic hapludox. DRI  $i_s$  ranged from 2.3 to 140  $\text{cm h}^{-1}$  while the CSI ranged from 1.3 to 30  $\text{cm h}^{-1}$ . The influence of added pressure head from ponded flow to measure DRI  $i_s$  was used to explain the results. Results from Zwirtes et al. (2013) do not agree with results from this study which may be explained by the methods used for calculating infiltration. A method involving the Kostiakov equation was used for calculating DRI infiltration and a runoff estimation method proposed by Carlesso et al. (2011) was adapted for the CSI measurements. Barrett and Rodgers



(2015) used a falling-head method for measuring DRI infiltration rate. Their study gave variable results for infiltration rate measured in a laboratory setting using three commercially available sands for both the CSI and DRI. Infiltration rates ranged from 32 to 58 cm h<sup>-1</sup> for the DRI and 44 to 94 cm h<sup>-1</sup> for the CSI. Measured infiltration rate averaged 4% greater for the CSI using one of the materials, whereas infiltration of the other two materials was 48 and 32% greater for the DRI. No consistent relationship between the two methods was found. Results and Barrett and Rodgers (2015) may not agree with results from this study because a falling head method was used for DRI measurements, and measuring  $i_s$  was not an objective of their study.

### **Layer $K_S$ Comparison**

The  $K_S$  values had greater overall variation than  $i_s$  from either measurement method across all sites (Table 2.4). Such variability is commonly observed in laboratory measurements of  $K_S$ , even after log transformations are performed (Lee et al., 1985; Mohanty et al., 1994; Reynolds et al., 2000), possibly due to the relatively small size of core samples. Four conditions had distinction between surface  $K_S$  and subsurface  $K_S$  at  $p = 0.05$ . These included SECREF N, CCRS T, JS TC, and JS N. For SECREF N conditions, surface  $K_S$  was less than subsurface  $K_S$ . Surface  $K_S$  varied substantially (CV >20%) for all but SECREF TC, CCRS T, CCRS F, JS TC, and LP N conditions. JS and LP subsurface  $K_S$  varied greatly (CV > 60.0% for all conditions). SECREF and CCRS sites had less subsurface  $K_S$  variability (CV < 20%). The variability in  $K_S$  could be attributed to the site-specific land use. Soil at JS was transported and subsequently compacted to form the off-ramp and soil at LP was likely shaped and graded to create the desired topographical contour. The fill material and simulated construction conditions at SECREF could have been muted by the established vegetation. CCRS was likely less drastically manipulated compared to the other sites, having only agricultural management practices applied to it.

### **Comparison of $i_S$ with Subsurface $K_S$**

To determine if  $i_S$  could be related to  $i_v$  using subsurface  $K_S$ , a linear regression of subsurface  $K_S$  was plotted with CSI and DRI  $i_S$  (Fig. 2.3). Correlation between CSI  $i_S$  and subsurface  $K_S$  was strong ( $R^2 = 0.87$ ). Likewise, correlation between DRI  $i_S$  and subsurface  $K_S$  ( $R^2 = 0.83$ ) was strong. Though subsurface  $K_S$  correlates strongly with  $i_S$ , there is distinct clustering of two groups. These groups correspond to tillage depth, where the lower  $i_S$  data cluster corresponds to 15 cm depth tillage and the higher  $i_S$  data cluster data corresponds to 30 cm tillage depth. This grouping suggests a possible effect from depth of the surface layer on observed  $i_S$ .

### **CONCLUSION**

The primary objective of this study was to compare two ring infiltrometer methods for measuring steady infiltration rate in layered soils. The CSI method gave slightly greater estimates of  $i_S$  than the DRI method in layered soil conditions. A linear regression between the two methods ( $R^2 = 0.79$ ) showed the CSI method gave 3% greater  $i_S$  values than the DRI for layered soils. Application of the texture-based correction factor decreased the difference between the two methods to 2%, though the correlation of the two did not change. The two methods gave similar results of  $i_S$  for assessment of layered soil infiltration rate.

The  $i_S$  for both methods strongly correlated with subsurface layer  $K_S$ . More detailed analysis is needed to further develop relationship of  $i_S$  from a ring to  $i_v$  in layered soils. Finding this relationship may give a practical understanding of how ring infiltrometer measurements can be related to infiltration events in layered soils and may give more precise evaluations of soil management practices.

## REFERENCES

- Ahuja, L.R., El-Swaify, S.A., Rahman, A., 1976. Measuring hydrologic properties of soil with a double-ring infiltrometer and multiple-depth tensiometers. *Soil Science Society of America Journal* 40, 494–499.
- ASTM, 2009. Standard test method for infiltration rate of soils in field using double-ring infiltrometer. ASTM International 10.
- Bagarello, V., Provenzano, G., 1996. Factors Affecting Field and Laboratory Measurement of Saturated Hydraulic Conductivity. *Transactions of the ASAE* 39, 153–159.
- Barrett, K.R., Rodgers, D., 2015. Laboratory measurements of infiltration capacity by a double ringed infiltrometer and the Cornell Sprinkle Infiltrator. *Water Practice and Technology* 10, 761–766.
- Blake, G.R., 1965. Bulk Density. *Methods of Soil Analysis. Part 1. Physical and Mineralogical Properties, Including Statistics of Measurement and Sampling* 374–390.
- Bouwer, H., 1986. Intake Rate: Cylinder Infiltrator. *Methods of Soil Analysis: Part 1—Physical and Mineralogical Methods* 825–844.
- Burgy, R.H., Luthin, J.N., 1956. A test of the single-and double-ring types of infiltrators. *Eos, Transactions American Geophysical Union* 37, 189–192.
- Carlesso, R., Spohr, R.B., Eltz, F.L.F., Flores, C.H., 2011. Runoff estimation in southern Brazil based on Smith's modified model and the Curve Number method. *Agricultural Water Management* 98, 1020–1026.
- Daniel, H.A., 1952. Recording Concentric Ring Infiltrator. *Agronomy Journal* 44, 451–451.

- Day, P.R., 1965. Particle Fractionation and Particle-Size Analysis. *Methods of Soil Analysis*. Part 1. Physical and Mineralogical Properties, Including Statistics of Measurement and Sampling Monogram, 545–567.
- Elrick, D.E., Angulo-Jaramillo, R., Fallow, D.J., Reynolds, W.D., Parkin, G.W., 2002. Infiltration under constant head and falling head conditions. *Environmental Mechanics: Water, Mass and Energy Transfer in the Biosphere: The Philip Volume* 47–53.
- Emerson, C.H., Traver, R.G., 2008. Multiyear and seasonal variation of infiltration from storm-water best management practices. *Journal of irrigation and drainage Engineering* 134, 598–605.
- Franzluebbers, A.J., Stuedemann, J.A., Franklin, D.H., 2012. Water infiltration and surface-soil structural properties as influenced by animal traffic in the Southern Piedmont USA. *Renewable Agriculture and Food Systems* 27, 256–265.
- Freeze, R.A., 1975. A stochastic-conceptual analysis of one-dimensional groundwater flow in nonuniform homogeneous media. *Water Resources Research* 11, 725–741.
- Haynes, M.A., McLaughlin, R.A., Heitman, J.L., 2013. Comparison of methods to remediate compacted soils for infiltration and vegetative establishment. *Open Journal of Soil Science* 3, 225.
- Hillel, D., 1998. *Environmental soil physics: Fundamentals, applications, and environmental considerations*. Academic press.
- Klute, A., Dirksen, C., 1986. Hydraulic conductivity and diffusivity: Laboratory methods. *Methods of Soil Analysis: Part 1—Physical and Mineralogical Methods* 687–734.

- Lee, D.M., Elrick, D.E., Reynolds, W.D., Clothier, B.E., 1985. A Comparison of Three Field Methods for Measuring Saturated Hydraulic Conductivity. *Canadian Journal of Soil Science* 65, 563–573.
- Liu, Y., Fu, B., Lü, Y., Wang, Z., Gao, G., 2012. Hydrological responses and soil erosion potential of abandoned cropland in the Loess Plateau, China. *Geomorphology* 138, 404–414.
- Maheshwari, B.L., 1996. Development of an automated double-ring infiltrometer. *Soil Research* 34, 709–714.
- Mohanty, B.P., Kanwar, R.S., Everts, C.J., 1994. Comparison of Saturated Hydraulic Conductivity Measurement Methods for a Glacial-Till Soil. *Soil Science Society of America Journal* 58, 672.
- Ogden, C.B., Van Es, H.M., Schindelbeck, R.R., 1997. Miniature rain simulator for field measurement of soil infiltration. *Soil Science Society of America Journal* 61, 1041–1043.
- Oliveira, M.T., Merwin, I.A., 2001. Soil physical conditions in a New York orchard after eight years under different groundcover management systems. *Plant and soil* 234, 233–237.
- Perkins, K.S., Nimmo, J.R., Medeiros, A.C., Szutu, D.J., von Allmen, E., 2014. Assessing effects of native forest restoration on soil moisture dynamics and potential aquifer recharge, Auwahi, Maui. *Ecohydrology*. 7, 1437–1451.
- Reynolds, W.D., Bowman, B.T., Brunke, R.R., Drury, C.F., Tan, C.S., 2000. Comparison of Tension Infiltrometer, Pressure Infiltrometer, and Soil Core Estimates of Saturated Hydraulic Conductivity. *Soil Science Society of America Journal* 64, 478.
- Reynolds, W.D., Elrick, D.E., 1990. Poned infiltration from a single ring: I. Analysis of steady flow. *Soil Science Society of America Journal* 54, 1233–1241.

- Reynolds, W.D., Elrick, D.E., Youngs, E.G., 2002. Single-ring and double-or concentric-ring infiltrometers. *Methods of soil analysis. Part 4*, 821–826.
- Swartzendruber, D., Olson, T.C., 1961. Sand-model study of buffer effects in the double-ring infiltrometer. *Soil Science Society of America Journal* 25, 5–8.
- Touma, J., Albergel, J., 1992. Determining soil hydrologic properties from rain simulator or double ring infiltrometer experiments: a comparison. *Journal of hydrology* 135, 73–86.
- van Es, H.M., Schindelbeck, R.R., 2003. Field procedures and data analysis for the Cornell sprinkle infiltrometer. *Department of Crop and Soil Science Research Series R03-01*.
- Verbist, K., Torfs, S., Cornelis, W.M., Oyarzún, R., Soto, G., Gabriels, D., 2010. Comparison of single-and double-ring infiltrometer methods on stony soils. *Vadose Zone Journal* 9, 462–475.
- Wilson, G.V., Luxmoore, R.J., 1988. Infiltration, Macroporosity, and Mesoporosity Distributions on Two Forested Watersheds. *Soil Science Society of America Journal* 52, 329.
- Wu, L., Pan, L., Roberson, M.J., Shouse, P.J., 1997. Numerical Evaluation of Ring-Intiltrometeres Under Various Soil Conditions. *Soil Science* 162, 771–777.
- Youngs, E.G., 1987. Estimating hydraulic conductivity values from ring infiltrometer measurements. *Journal of Soil Science* 38, 623–632.
- Zwirtes, A.L., Spohr, R.B., Baronio, C.A., Menegol, D.R., da Rosa, G.M., de Moraes, M.T., 2013. Soil water infiltration measurements using the double ring and Cornell infiltrometer in a Rhodic Hapludox. *Semina: Ciências Agrárias (Londrina)* 34, 3489–3499.

**Table 2.1. Soil texture for layered materials at four sites.**

Soil Layer	Particle Size Distribution			Texture
	Sand	Silt	Clay	
———— % ————				
<u>Sediment and Erosion Control Research and Extension Facility (SECREF)</u>				
Surface (0-30 cm)	46.8	19.8	33.4	Sandy Clay Loam
Subsurface (>30 cm)	39.4	21.2	39.4	Clay Loam
<u>Central Crops Research Station (CCRS)</u>				
† Surface (0-30 cm)	94.7	4.7	0.6	Sand
† Subsurface (>30 cm)	86.0	8.3	5.7	Loamy Sand
‡ Surface (0-30 cm)	87.8	11.0	1.2	Loamy Sand
‡ Subsurface (>30 cm)	86.6	11.8	1.6	Loamy Sand
<u>Jones Sausage Rd. highway off-ramp (JS)</u>				
Surface (0-15 cm)	56.1	27.4	16.5	Sandy Loam
Subsurface (>15 cm)	61.2	20.2	18.6	Sandy Loam
<u>Lonnie Poole Golf Course (LP)</u>				
Surface (0-15 cm)	47.1	22.8	30.0	Sandy Clay Loam
Subsurface (>15 cm)	42.9	19.9	37.1	Clay Loam

† Field was tilled and between rotations.

‡ Fallow hayfield.

**Table 2.2. Site management practices and bulk density by depth for surface and subsurface materials.**

Site	Management Practice	Tillage Depth cm	Bulk Density			
			Surface Material			Subsurface Material†
			0-7.5 cm	7.5-15.0 cm	15.0-22.5 cm	
			<b>g cm<sup>-3</sup></b>			
SECREF‡	Tillage (T)	30	1.41 (± 0.09)	1.42 (± 0.17)	1.49 (± 0.11)	1.53 (± 0.18)
	Tillage, gypsum incorporated (TG)		1.30 (± 0.06)	1.35 (± 0.11)	1.40 (± 0.13)	1.49 (± 0.11)
	Tillage, compost incorporated (TC)		1.16 (± 0.06)	1.26 (± 0.19)	1.38 (± 0.05)	1.49 (± 0.26)
	Tillage, polyacrylamide incorporated (TP)		1.34 (± 0.04)	1.39 (± 0.09)	1.49 (± 0.11)	1.38 (± 0.11)
	No management practice (N)	—	1.55 (± 0.05)	1.59 (± 0.03)	1.60 (± 0.07)	1.47 (± 0.13)
CCRS	Tillage (T)	30	1.44 (± 0.05)	—	—	1.83 (± 0.06)
	Fallow (F)	—	1.45 (± 0.04)	—	—	1.78 (± 0.07)
JS	Tillage (T)	15	1.41 (± 0.09)	—	—	1.74 (± 0.11)
	Tillage, compost incorporated (TC)		1.22 (± 0.05)	—	—	1.69 (± 0.11)
	Previous management practice (N)	—	1.62 (± 0.07)	—	—	1.74 (± 0.11)
LP	Tillage (T)	15	1.39 (± 0.10)	—	—	1.48 (± 0.16)
	Tillage, compost incorporated (TC)		1.16 (± 0.02)	—	—	1.48 (± 0.16)
	Previous management practice (N)	—	1.46 (± 0.11)	—	—	1.53 (± 0.02)

† Subsurface material represents material below tillage depth.

‡ Samples were collected at multiple 7.5 cm increments in surface material.



**Table 2.3. Comparison of steady infiltration rate ( $i_s$ ) values measured using Cornell Sprinkle Infiltrometer (CSI) and ASTM double-ring infiltrometer (DRI) methods.**

Site	Management Practice	CSI				DRI				$p^{\parallel}$
		$i_{GM}^{\dagger}$	$i_{AR}^{\ddagger}$	Range	CV $^{\S}$	$i_{GM}$	$i_{AR}$	Range	CV	
		— log 10 <sup>-4</sup> m day <sup>-1</sup> —				— log 10 <sup>-4</sup> m day <sup>-1</sup> —				
SECREF	Tillage (T)	4.67	4.69	4.05-5.03	9.84	4.99	4.99	4.61-5.44	6.88	0.33
	Tillage, gypsum incorporated (TG)	4.95	4.95	4.78-5.10	2.68	5.02	5.03	4.86-5.25	3.22	0.52
	Tillage, compost incorporated (TC)	4.89	4.89	4.79-5.00	3.98	5.20	5.20	4.97-5.30	3.02	0.05*
	Tillage, polyacrylamide incorporated (TP)	4.85	4.85	4.61-5.00	3.91	4.70	4.71	4.44-5.04	5.74	0.43
	No management practice (N)	4.08	4.09	3.78-4.60	8.92	1.53	2.51	0.16-3.62	<b>64.1</b>	0.10
CCRS	Tillage (T)	4.37	4.37	4.12-4.73	4.30	4.22	4.22	4.01-4.43	4.50	0.39
	Fallow (F)	4.62	4.63	4.33-4.77	5.90	4.27	4.28	4.01-4.56	5.30	0.06
JS	Tillage (T)	3.68	3.69	3.29-3.99	7.87	1.32	2.06	0.16-3.29	<b>65.1</b>	0.78
	Tillage, compost incorporated (TC)	4.07	4.07	3.87-4.40	5.63	3.60	3.62	3.16-4.10	10.8	0.26
	Previous management practice (N)	3.99	4.00	3.76-4.17	4.75	1.11	1.66	0.16-2.77	<b>66.0</b>	0.01*
LP	Tillage (T)	3.43	3.44	3.22-3.76	6.97	3.24	3.30	2.53-4.00	20.8	0.71
	Tillage, compost incorporated (TC)	3.75	3.77	3.30-4.41	12.4	3.50	3.53	2.96-4.14	16.2	0.55
	Previous management practice (N)	0.74	1.80	0.16-3.64	<b>106</b>	1.39	2.22	0.16-3.45	<b>65.4</b>	0.78

\*Significant at 0.05 probability. Arithmetic means were used to test significance.

$\dagger$  Geometric mean.

$\ddagger$  Arithmetic mean.

$\S$  Coefficient of variation.  $i_{AR}$  was used in calculating CV.

$\parallel$  Statistical difference between  $i_s$  measurements based on  $i_{AR}$ .

CV values in bold represent conditions with high  $i_s$  variability.

**Table 2.4. Saturated hydraulic conductivity ( $K_S$ ) values for surface and subsurface materials.**

Site	Management Practice	Surface Material				Subsurface Material				$p^{\parallel}$
		$K_{GM}^{\dagger}$	$K_{AR}^{\ddagger}$	Range	CV $^{\S}$	$K_{GM}$	$K_{AR}$	Range	CV	
		— log 10 <sup>-4</sup> m day <sup>-1</sup> —				— log 10 <sup>-4</sup> m day <sup>-1</sup> —				
		%				%				
SECREF#	Tillage (T)	2.30	3.06	0.48-4.50	60.2	3.82	3.85	3.16-4.44	13.9	0.44
	Tillage, gypsum incorporated (TG)	3.00	3.24	1.64-4.40	41.4	3.73	3.76	2.98-4.15	14.1	0.50
	Tillage, compost incorporated (TC)	4.68	4.73	3.75-5.58	16.3	3.97	3.98	3.71-4.35	7.53	0.12
	Tillage, polyacrylamide incorporated (TP)	2.30	2.59	1.50-5.00	62.5	3.89	3.99	2.75-5.13	25.5	0.19
	No management practice (N)	1.61	2.03	0.62-3.40	69.0	4.11	4.12	3.88-4.69	9.33	0.03*
CCRS	Tillage (T)	4.88	4.88	4.83-4.91	0.80	3.60	3.66	2.66-4.28	19.0	0.01*
	Fallow (F)	4.52	4.53	4.19-4.87	7.20	3.79	3.83	3.10-4.60	16.2	0.09
JS $^{\dagger\dagger}$	Tillage (T)	3.05	3.47	1.13-4.64	45.9	1.04	1.51	0.16-2.22	60.9	0.08
	Tillage, compost incorporated (TC)	4.55	4.56	4.17-4.99	7.78	1.32	2.18	0.16-3.91	75.8	0.03*
	Previous management practice (N)	2.83	2.88	2.34-3.65	21.2	1.04	1.51	0.16-2.22	60.9	0.05*
LP $^{\dagger\dagger}$	Tillage (T)	3.39	3.64	1.85-5.03	40.4	0.75	1.88	0.16-3.97	107	0.21
	Tillage, compost incorporated (TC)	3.80	3.89	2.60-4.74	23.6	0.75	1.88	0.16-3.97	107	0.54
	Previous management practice (N)	3.61	3.62	3.23-4.16	10.8	0.52	3.02	0.16-4.35	67.2	0.07

\*Significant at 0.05 probability level. Arithmetic means were used to test significance.

$^{\dagger}$  Geometric mean.

$^{\ddagger}$  Arithmetic mean.

$^{\S}$  Coefficient of variation.  $K_{AR}$  was used in calculating CV.

$^{\parallel}$  Statistical difference between surface and subsurface  $K_S$  based on  $K_{AR}$ .

# Values for surface material represent effective  $K_S$ , measured for depths of 0 to 7.5 cm, 7.5 to 15.0 cm, and 15.0 to 22.5 cm.

$^{\dagger\dagger}$  Individual measurements were not made from each plot to characterize subsurface conditions.

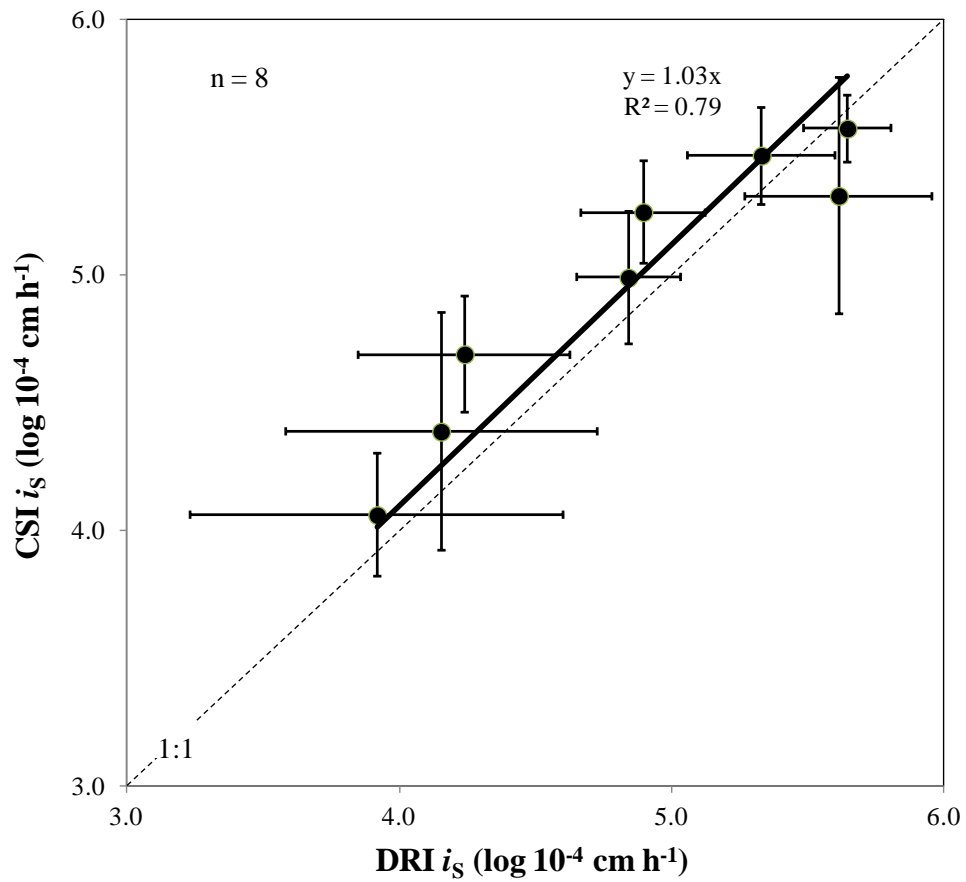


**Figure 2.1.** Linear regression of ASTM double-ring infiltrometer (DRI) steady infiltration rate ( $i_s$ ) versus Cornell Sprinkle Infiltrometer (CSI)  $i_s$  for layered conditions. Points are geometric means of  $i_s$  for each set of conditions. Error bars are one standard deviation from the mean.

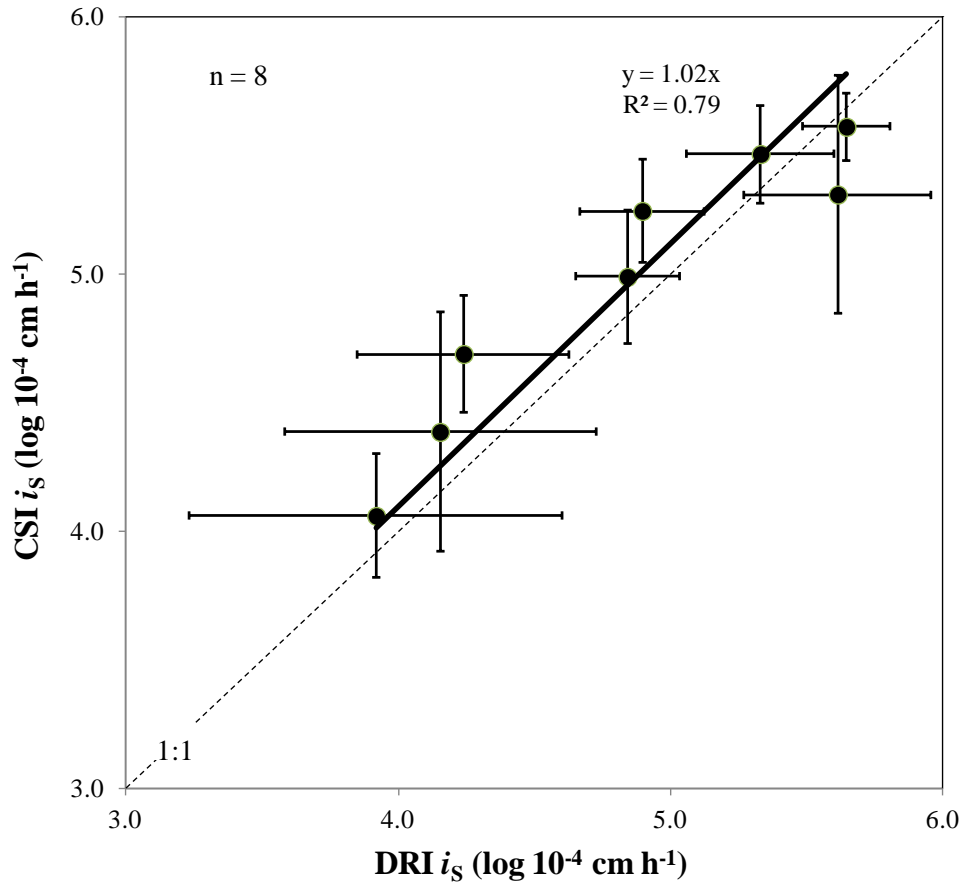


**Figure 2.2.** Linear regression of ASTM double-ring infiltrometer (DRI) steady infiltration rate ( $i_s$ ) versus Cornell Sprinkle Infiltrometer (CSI)  $i_s$  with texture-based correction applied for CSI measurements. Points are geometric means of  $i_s$  for each set of conditions. Error bars are one standard deviation from the mean.

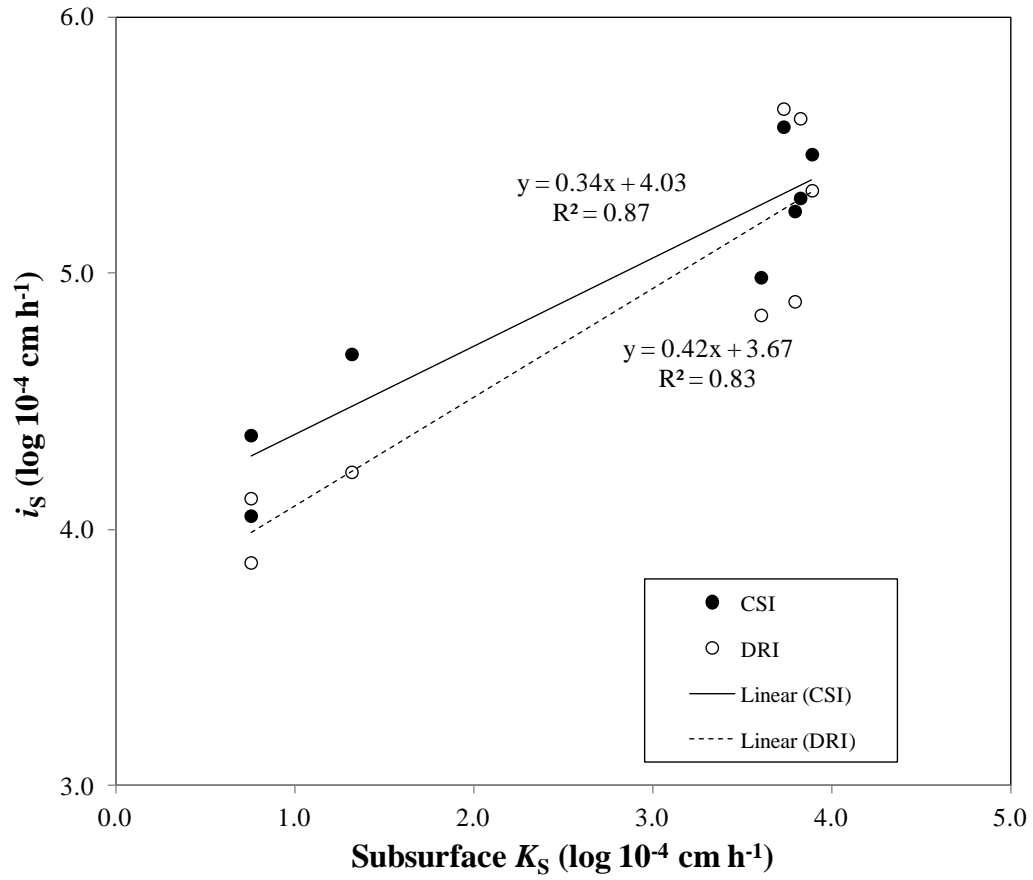


**Figure 2.3.** Linear regressions of steady infiltration rate ( $i_s$ ) measured using the Cornell Sprinkle Infiltrometer (CSI) and ASTM double-ring infiltrometer (DRI) methods versus saturated hydraulic conductivity ( $K_S$ ) for subsurface layers.

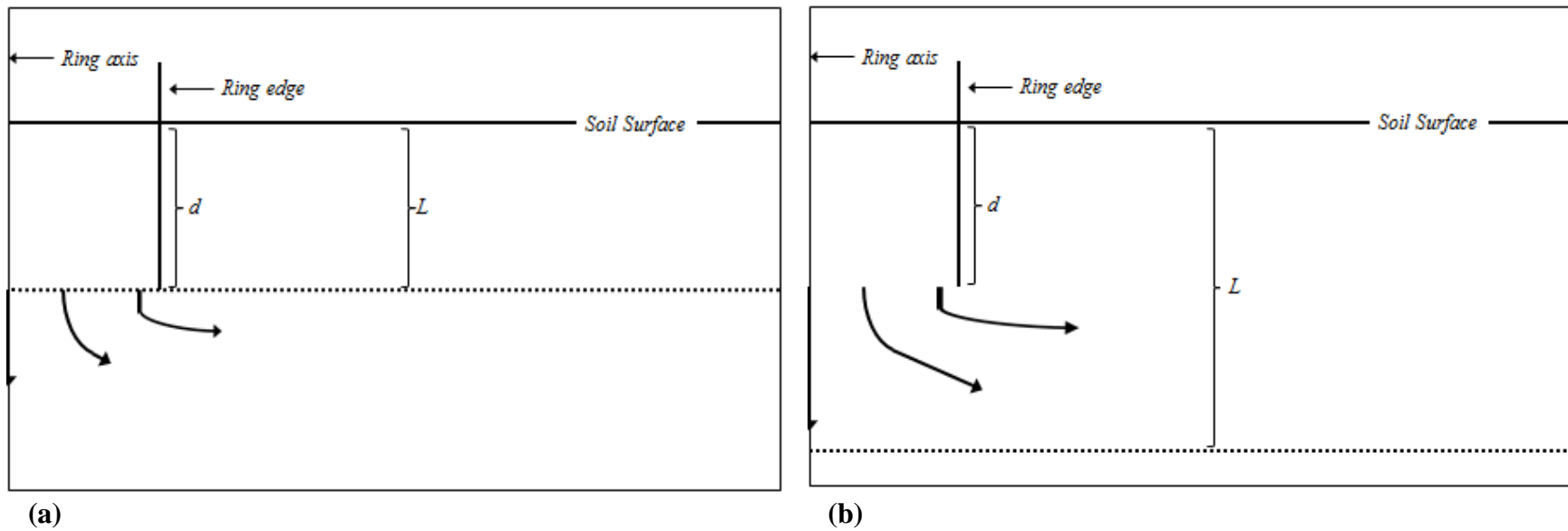


**Figure 2.4.** Axisymmetric schematics of experimental conditions from ring infiltrometer measurements in layered soil.

Depths to subsurface layer ( $L$ ) equal to 15 cm (a) and 30 cm (b). Ring depth ( $d$ ) = 15 cm. Dotted line represents layer boundary.

### Chapter 3: Numerical Assessment of a Single-ring Sprinkle Infiltrometer Method for Measuring Steady Infiltration Rate of Layered Soils

#### ABSTRACT

Land management practices designed to improve infiltration can create layered soil conditions, where a more hydraulically conductive surface layer overlays a less conductive subsurface layer. Steady infiltration rate measured using ring infiltrometers ( $i_S$ ) is frequently used to evaluate these practices. Methods of measuring  $i_S$  using ponded flow may not be consistent with naturally occurring infiltration processes. Single-ring sprinkle infiltrometer methods may give more representative results with respect to natural infiltration processes because they allow partitioning of rainfall to infiltration and runoff (without ponding), but the single-ring component may be affected by lateral flow. The objective of this study was to determine how soil layering influences  $i_S$  measured using the Cornell Sprinkle Infiltrometer method. Experimentally validated simulations using conditions from two case studies were performed in HYDRUS 2D to test the effects of depth to impeding subsurface layer and contrast in layer saturated hydraulic conductivities ( $K_S$ ) on  $i_S$  relative to vertical infiltration rate with one-dimensional flow ( $i_v$ ). Results show that depth to impeding subsurface layer can affect measured  $i_S$  relative to  $i_v$  ( $i_S/i_v$ ), and that this effect reaches some depth-dependent maximum depending on contrast in surface and subsurface layer  $K_S$ . For the two cases tested,  $i_S/i_v$  approached values as large as 67.1 when layer  $K_S$  contrast was greater than one order of magnitude, and  $i_S/i_v$  was small (1.0 to 15.7) when contrast was one order of magnitude or less. These results indicate that  $i_S$  can give an exaggerated estimate of the infiltration rate for management practices that create layered soil conditions if there are substantial differences (greater than an order of magnitude) in surface and subsurface  $K_S$ .

## INTRODUCTION

Infiltrometer measurements are often used to assess practices designed to improve soil infiltration, and the observed steady infiltration rate ( $i_s$ ) is commonly used for the evaluation. Ring infiltrometers with ponded infiltration, where observed infiltration rate is dependent upon the height of the column of water, are among the most common methods used to measure  $i_s$ . These measurements can be cumbersome and time-consuming (Elrick et al., 2002; Maheshwari, 1996). Another approach, the Cornell Sprinkle Infiltrometer (CSI) method (Ogden et al., 1997), has been used with increasing frequency to determine infiltration rates (Alizadehtazi et al., 2016; Edgell et al., 2015; Haynes et al., 2013; Oliveira and Merwin, 2001). The CSI may be preferable to ponded methods of measuring infiltration because it incorporates a mini-rainfall simulator to mimic surface rainfall partitioning without forcing ponding. The apparatus is also mostly self-contained, making field measurements more convenient than other measurement methods (van Es and Schindelbeck, 2003).

Management practices intended to improve soil infiltration rate often involve disruption of the surface through tillage and vegetation establishment to encourage the development of soil structure. Disruption of the soil surface creates a layering effect, where a more conductive, less dense surface layer may overlay a less conductive, denser subsurface layer. This subsurface layer may influence the infiltration rate observed using an infiltrometer by increasing lateral flow at the layer boundary (Bouwer, 1986; Hillel, 1998). The effects of soil layering on  $i_s$  can be tested numerically. Using numerical simulations, Wu et al. (1997) showed that shallow depths to changes in layer texture increased the deviation of infiltrometer measurements from vertical infiltration rate, and depth to layering also influenced the time at which the measurements deviated. We hypothesized that the CSI, a single-ring approach, may be particularly susceptible



to lateral flow affects, compared to more commonly used double-ring infiltrometer approaches (Reynolds et al., 2002; Swartzendruber and Olson, 1961; Youngs, 1987).

The objective of this study was to determine the influence of soil layering on  $i_s$  measured using CSI method relative to vertical one-dimensional infiltration rate ( $i_v$ ). Numerical tests were used to assess soil layering effects. The effects tested included depth to limiting subsurface layer and the contrast in saturated hydraulic conductivity between layers. It was hypothesized that effects from soil layering would cause lateral flow to exaggerate CSI final infiltration rates compared to actual one-dimensional infiltration.

## **MATERIALS AND METHODS**

### **Infiltration Measurements**

Two sites with distinctly different soil conditions were selected to assess the infiltrometer measurements. A fallow agricultural field located at the Central Crops Research Station in Clayton, NC was tilled to a depth of 30 cm (CCRS). A plot-scale study located at the Lonnie Poole Golf Course in Raleigh, NC was tilled to a depth of 15 cm with compost incorporated (LP). NRCS map units were Norfolk Loamy Sand for CCRS measurements and Cecil Sandy Loam for LP measurements.

Infiltration measurements were made at each site according to the method outlined in the CSI manual (van Es and Schindelbeck, 2003). The CSI consists of a miniature rainfall simulator combined with a single ring. The ring has a hole in its exterior, positioned flush with the soil surface at installation, which prevents ponding by allowing surface runoff. “Runoff” from within the ring is collected through a tube affixed to the hole. Infiltration is measured by taking the difference between the volume of water applied by the rainfall simulator and the volume of runoff exiting the ring per unit time. Ring diameter was 24.1 cm and ring depth was

15 cm. Rainfall rate was between 0.7 and 0.9 cm min<sup>-1</sup> for CCRS and between 0.5 and 0.7 cm min<sup>-1</sup> for LP. Rainfall and runoff were recorded at one-minute intervals. The  $i_s$  was assumed to have been reached when ten consecutive runoff measurements varied by less than 0.42 cm min<sup>-1</sup>, corresponding to 10 mL volume over the collection area.

### **Soil Property Measurements**

Samples were collected at each site to determine properties from individual soil layers. Soil hydraulic properties including saturated hydraulic conductivity ( $K_s$ ) and water retention were measured from samples collected at each infiltration measurement position. Samples (7.5 cm in diameter and 7.5 cm in height) were collected using a Uhland core sampler and measured for bulk density (Blake, 1965). Cores were weighed before and after oven drying (105 °C) to determine volumetric water content. Saturated hydraulic conductivity was measured on intact samples using a benchtop constant head method (Klute and Dirksen, 1986). Particle density was measured using an air pycnometer (Flint and Flint, 2002). Soil texture was determined by the hydrometer method (Day, 1965). Porosity was calculated from measured particle density and bulk density of each sample. Soil water retention was measured at 100, 330, 500, 1,000, 5,000, and 15,000 cm using a pressure plate method (Klute, 1986). Water retention measurements were fitted to the van Genuchten water retention model (van Genuchten, 1980) using the RETC program (van Genuchten et al., 1991). Soil material properties are summarized in Table 3.1.

### **Numerical Simulations and Validation**

CSI measurements and rainfall events were simulated using HYDRUS 2D (Simunek et al., 2006) for a 60-min. duration. HYDRUS 2D is a modeling software package that numerically solves the Richards Equation for flow in two dimensions using a finite element method. An axisymmetric domain geometry similar to Lai et al. (2010) was used for ring infiltrometer

simulations (Fig. 3.1). The domain width was 100 cm and the total depth was adjusted to ensure  $i_s$  was reached within the 60 minute simulation, varying between 100 and 200 cm. CSI depth extended to 15 cm and ring radius was 12 cm. Finite element mesh size was 1.0 cm with a mesh refinement of 1.5 cm at the lower boundary. The upper boundary condition was an atmospheric boundary with precipitation set to the average rainfall from the infiltrometer measurement. This atmospheric boundary was used within the 12 cm ring radius for the infiltrometer simulations and spanned the entire upper boundary of the domain for the precipitation simulations. Lower boundary conditions were set to free drainage. Initial conditions were approximated based on measured volumetric water contents. Simulation inputs were  $\theta_r$ ,  $\theta_s$ ,  $\alpha$ , and  $n$  parameters from the fitted water retention curves using the van Genuchten function (van Genuchten, 1980) and  $K_S$  measured in the laboratory (Table 3.1). Selected numerical simulation information and domain properties are summarized in Table 3.2.

The HYDRUS simulations were based on experimentally derived parameters (field measurements) and therefore did not require calibration (Simunek et al., 2012). Model agreement to measurements was improved by adjusting depth to subsurface layer ( $L$ ) for both cases. Values for  $L$  were based on the maximum depth of tillage for each condition (Chapter 2). Simulation infiltration rate and cumulative infiltration curves were plotted with the corresponding field measurement results for CCRS and LP conditions in Figure 3.2. For CCRS, simulated  $i_s$  was  $0.32 \text{ cm min}^{-1}$  and simulated cumulative infiltration was 13.6 cm. These values were within the ranges measured for CCRS conditions as reported in Chapter 2 ( $0.15$  to  $0.41 \text{ cm min}^{-1}$  and  $10.5$  to  $15.0 \text{ cm}$  for  $i_s$  and cumulative infiltration, respectively). For LP, simulated  $i_s$  was  $0.15 \text{ cm min}^{-1}$  and simulated cumulative infiltration was 4.12 cm. These values were also within the ranges measured ( $0.003 \text{ cm min}^{-1}$  to  $0.38 \text{ cm min}^{-1}$  and  $1.54$  to  $53.7 \text{ cm}$  for  $i_s$  and

cumulative infiltration, respectively; see Chapter 2). Overall, agreement between simulations and measurements was strong.

### **Analyses**

The effects from  $L$  and degree of contrast between layer  $K_S$  values were tested in HYDRUS 2D for CCRS and LP. Simulations were performed where  $L$  values were adjusted incrementally (1 cm increments at 0 to 10 cm, 5 cm increments at 10 to 30 cm, and 10 cm increments at >30cm) to simulate varying surface layer thickness. Combinations of different  $K_S$  values for surface and subsurface layers were used to test the effect of contrasting layer conductivity. A range of surface  $K_S$  values was used in combination with three fixed subsurface  $K_S$  values. The fixed subsurface  $K_S$  values were 0.05, 0.005 and 0.0005  $\text{cm min}^{-1}$  for CCRS and 0.07, 0.007, and 0.0007  $\text{cm min}^{-1}$  for LP. These values represent the measured subsurface  $K_S$  from each field site and the measured values reduced by factors of 10 and 100. These reductions in subsurface conductivity were used to represent extreme conditions with significant layer contrasts relative to measured conditions in the field. Simulation flux (infiltration) rates were averaged over the final ten minutes to obtain  $i_S$  and  $i_v$ , in accordance with the method used to obtain  $i_S$  for field experiments. Only combinations where  $i_S$  was attained (i.e., observed infiltration rate was no longer trending downward) during the 60 minute simulation were used for analysis. Simulated conditions included surface  $K_S$  values that ranged from 0.07 to 1.12  $\text{cm min}^{-1}$  for CCRS and 0.03 to 0.52  $\text{cm min}^{-1}$  for LP, paired with the chosen subsurface  $K_S$  values. Example simulations showing water content distributions at the steady-state conditions and their associated infiltration rate curves are shown in Figure 3.3. All analyzed simulations had less than 0.01  $\text{cm min}^{-1}$  change in rate over the final ten minutes.

## RESULTS AND DISCUSSION

### Depth Effect on Infiltrometer Measurement

The effects of layer depth were tested using hydraulic properties measured in the field for HYDRUS 2D simulations. Results for CCRS and LP both showed that  $i_s$  is exaggerated relative to  $i_v$  with increasing  $L$  (Fig. 3.4). Both cases also show that  $i_s$  was most similar to  $i_v$  (i.e.,  $i_s/i_v = 1$ ) when the material distribution was completely homogeneous (i.e., soil properties were uniform with depth). The  $i_s/i_v$  was 1.06 and 1.08 at  $L = 0$  (i.e., subsurface properties make up the whole profile) and  $L = 200$  cm (i.e., surface properties make up the whole profile), respectively, for CCRS (Fig. 3.4). The  $i_s/i_v$  was 1.13 and 1.12 at  $L = 0$  and  $L = 200$  cm, respectively, for LP (Fig. 3.4). This can be explained by vertical, gravity-driven flow being dominant to lateral flow once steady infiltration was achieved, allowing for a quasi-steady flow similar to  $i_v$  (Wooding, 1968). In practical terms this indicates that the sprinkle infiltrometer is expected to provide a reasonable estimate of steady vertical infiltration rate over the range of hydraulic property conditions represented by surface and subsurface properties in CCRS and LP (e.g.,  $K_S$  ranging from 0.56 to 0.05 cm min<sup>-1</sup>), if soil properties are uniform with depth. Exaggeration begins to sharply increase when  $L = 10$  cm (Fig. 3.4). A maximum deviation was reached for the two cases at differing depths. The maximum deviation also differed; deviation was greater for CCRS than LP, with  $i_s/i_v$  of 6.38 at  $L = 50$  cm for CCRS and  $i_s/i_v$  of 1.78 at  $L = 30$  cm for LP (Fig. 3.4). These conditions represent the maximum deviation (i.e., largest  $i_s/i_v$ ) for each case.

CCRS had saturated hydraulic conductivity an order of magnitude greater in the surface layer (0.56 cm min<sup>-1</sup>) compared to the subsurface layer (0.05 cm min<sup>-1</sup>), while LP had approximately twice as great a saturated hydraulic conductivity in the surface layer (0.13 cm min<sup>-1</sup>) compared to the subsurface layer (0.07 cm min<sup>-1</sup>). This indicates that depth to impeding

subsurface layer is an important factor in relating  $i_s$  measured using a ring infiltrometer to  $i_v$  but that the depth where most deviation occurs depends on contrast in layer  $K_S$ . For instance, at  $L = 30$  cm the maximum deviation for LP is reached, while the deviation for CCRS continues increasing (Fig. 3.4). The  $i_s/i_v$  is also greater for CCRS (5.31) than LP (1.78) at  $L = 30$  (Fig. 3.4). This is because greater surface  $K_S$  allows for more lateral flow and greater exaggeration with respect to  $i_v$ . When surface  $K_S$  values are closer to subsurface  $K_S$  values, exaggeration will be minimal and layering effects on  $i_s$  will also be minimal, regardless of  $L$ .

### **Contrasting Layer $K_S$ Effect on Infiltration Measurement**

Contrast in layer  $K_S$  was also tested numerically. CCRS and LP both show increasing  $i_s/i_v$  as surface  $K_S$  increases for the three fixed subsurface  $K_S$  values (Fig. 3.5 and Fig. 3.6). CCRS had a range of 1.06 to 5.9 for  $i_s/i_v$  when subsurface  $K_S$  is  $0.05 \text{ cm min}^{-1}$ , a range of 1.97 to 19.8 when subsurface  $K_S$  is  $0.005 \text{ cm min}^{-1}$ , and a range of 5.96 to 67.1 when subsurface  $K_S$  is  $0.0005 \text{ cm min}^{-1}$  (Fig. 3.5). LP had a range of 1.0 to 4.5 for  $i_s/i_v$  when subsurface  $K_S$  is  $0.07 \text{ cm min}^{-1}$ , a range of 1.4 to 15.7 when subsurface  $K_S$  is  $0.007 \text{ cm min}^{-1}$ , and a range of 4.1 to 37.3 when subsurface  $K_S$  is  $0.0007 \text{ cm min}^{-1}$  (Fig. 3.6). Exaggeration was most extreme when subsurface  $K_S$  was lowest for both cases. Layer  $K_S$  combinations where contrast was greater than one order of magnitude ranged 12.3 to 67.1 over both cases. These results show that  $i_s$  may potentially be, at minimum, 1200% greater than  $i_v$  when subsurface  $K_S$  is low ( $10^{-4} \text{ cm min}^{-1}$ ). Layer  $K_S$  combinations where contrast was within one order of magnitude, however, gave  $i_s/i_v$  that ranged from 1.0 to 15.7 over both cases. Since  $i_s$  for CSI and double-ring measurements were similar (Chapter 2), comparable results could be expected for double-ring methods. Overall, simulation results indicate that care must be taken when interpreting infiltrometer results when there is substantial contrast in surface and subsurface hydraulic conductivity. However,

when the contrast is small (within one order of magnitude), infiltrometer results approached a value similar to simple one-dimensional vertical infiltration.

## CONCLUSION

The effects of soil layering on  $i_s$  measured from a CSI were tested using simulations in HYDRUS 2D. Simulations were validated from field experiments using the CSI method. The results indicate that layered conditions exaggerate  $i_s$  from a ring infiltrometer relative to  $i_v$ . Depth to impeding subsurface layer is one factor that affects  $i_s$  from a ring infiltrometer relative to  $i_v$ . This effect reaches a maximum at some depth dependent upon degree of contrast in layer  $K_S$ . This depth is shallower the closer surface  $K_S$  values are to subsurface  $K_S$  values, implying that ring infiltrometer measurements used to evaluate practices that create different layer depths may not be comparable to one another. As surface  $K_S$  increases, influence of subsurface  $K_S$  on  $i_s$  becomes greater, with increasing lateral flow as subsurface  $K_S$  decreases. When hydraulic properties differ slightly between surface and subsurface conditions, infiltrometer infiltration rates do, however, approach values similar to one-dimensional vertical infiltration. Further research to determine which factors can relate  $i_s$  from ring infiltrometer measurements to  $i_v$  in layered soils may lead to more effective evaluations of management practices that create layered soil conditions.

## REFERENCES

- Alizadehtazi, B., DiGiovanni, K., Foti, R., Morin, T., Shetty, N.H., Montalto, F.A., Gurian, P.L., 2016. Comparison of Observed Infiltration Rates of Different Permeable Urban Surfaces Using a Cornell Sprinkle Infiltrometer. *Journal of Hydrologic Engineering* 6016003.
- Blake, G.R., 1965. Bulk Density. *Methods of Soil Analysis. Part 1. Physical and Mineralogical Properties, Including Statistics of Measurement and Sampling* 374–390.
- Bouwer, H., 1986. Intake Rate: Cylinder Infiltrometer. *Methods of Soil Analysis: Part 1—Physical and Mineralogical Methods*, 825–844.
- Day, P.R., 1965. Particle Fractionation and Particle-Size Analysis. *Methods of Soil Analysis. Part 1. Physical and Mineralogical Properties, Including Statistics of Measurement and Sampling Monogram*, 545–567.
- Edgell, J., Osmond, D.L., Line, D.E., Hoyt, G.D., Grossman, J.M., Larsen, E.M., 2015. Comparison of Surface Water Quality and Yields from Organically and Conventionally Produced Sweet Corn Plots with Conservation and Conventional Tillage. *Journal of Environment Quality* 44, 1861.
- Elrick, D.E., Angulo-Jaramillo, R., Fallow, D.J., Reynolds, W.D., Parkin, G.W., 2002. Infiltration under constant head and falling head conditions. *Environmental Mechanics: Water, Mass and Energy Transfer in the Biosphere: The Philip Volume* 47–53.
- Flint, A.L., Flint, L.E., 2002. 2.2 Particle Density. *Methods of Soil Analysis: Part 4 Physical Methods sssabookseries*, 229–240.
- Haynes, M.A., McLaughlin, R.A., Heitman, J.L., 2013. Comparison of methods to remediate compacted soils for infiltration and vegetative establishment. *Open Journal of Soil Science* 3, 225.



- Hillel, D., 1998. Environmental soil physics: Fundamentals, applications, and environmental considerations. Academic press.
- Klute, A., 1986. Water Retention: Laboratory Methods. *Methods of Soil Analysis: Part 1—Physical and Mineralogical Methods* 635–662.
- Klute, A., Dirksen, C., 1986. Hydraulic conductivity and diffusivity: Laboratory methods. *Methods of Soil Analysis: Part 1—Physical and Mineralogical Methods* 687–734.
- Lai, J., Luo, Y., Ren, L., 2010. Buffer index effects on hydraulic conductivity measurements using numerical simulations of double-ring infiltration. *Soil Science Society of America Journal* 74, 1526–1536.
- Maheshwari, B.L., 1996. Development of an automated double-ring infiltrometer. *Soil Research* 34, 709–714.
- Ogden, C.B., Van Es, H.M., Schindelbeck, R.R., 1997. Miniature rain simulator for field measurement of soil infiltration. *Soil Science Society of America Journal* 61, 1041–1043.
- Oliveira, M.T., Merwin, I.A., 2001. Soil physical conditions in a New York orchard after eight years under different groundcover management systems. *Plant and soil* 234, 233–237.
- Reynolds, W.D., Elrick, D.E., Youngs, E.G., 2002. Single-ring and double-or concentric-ring infiltrometers. *Methods of soil analysis. Part 4*, 821–826.
- Simunek, J., Genuchten, M., Sejna, M., 2012. HYDRUS: model use, calibration, and validation. *Transactions of the ASABE* 55, 1261–1274.
- Simunek, J., Van Genuchten, M.T., Sejna, M., 2006. The HYDRUS software package for simulating two and three-dimensional movement of water, heat, and multiple solutes in variably-saturated media. Technical manual 1.

- Soil Survey Staff, Natural Resources Conservation Service, United States Department of Agriculture. Web Soil Survey. Available online at <http://websoilsurvey.nrcs.usda.gov/>. Accessed July/13/2016.
- Swartzendruber, D., Olson, T.C., 1961. Sand-model study of buffer effects in the double-ring infiltrometer. *Soil Science Society of America Journal* 25, 5–8.
- van Es, H.M., Schindelbeck, R.R., 2003. Field procedures and data analysis for the Cornell sprinkle infiltrometer. Department of Crop and Soil Science Research Series R03-01.
- van Genuchten, M.T., 1980. A closed-form equation for predicting the hydraulic conductivity of unsaturated soils. *Soil science society of America journal* 44, 892–898.
- van Genuchten, M.T., Leij, F.J., Yates, S.R., others, 1991. The RETC code for quantifying the hydraulic functions of unsaturated soils.
- Wooding, R.A., 1968. Steady Infiltration from a Shallow Circular Pond. *Water Resources Research* 4, 1259–1273.
- Wu, L., Pan, L., Roberson, M.J., Shouse, P.J., 1997. Numerical evaluation of ring-infiltrimeters under various soil conditions. *Soil Science* 162, 771–777.
- Youngs, E.G., 1987. Estimating hydraulic conductivity values from ring infiltrometer measurements. *Journal of Soil Science* 38, 623–632.

**Table 3.1.** Soil material properties and inputs for two case studies.

<b>Layer</b>	<b>Texture</b>	<b>Bulk Density</b> $\text{g cm}^{-3}$	<b><math>K_S</math></b> $\text{cm min}^{-1}$	<b>van Genuchten Parameters</b>			
				$\theta_r$	$\theta_s$	$\alpha$	$n$
			<u>Case 1</u>				
<b>Surface</b>	Sand	1.50	0.56	0.003	0.432	1.242	1.359
<b>Subsurface</b>	Loamy Sand	1.84	0.05	0	0.308	0.226	1.264
			<u>Case 2</u>				
<b>Surface</b>	Sandy Clay Loam	1.17	0.13	0.01	0.59	0.05	1.18
<b>Subsurface</b>	Clay Loam	1.28	0.07	0	0.61	0.04	1.16

**Table 3.2.** Selected input parameters and domain information for numerical simulations.

	<b>Rainfall Rate</b>	<b>Layer Boundary Depth</b>	<b>Initial <math>h</math></b>
	<b>cm min<sup>-1</sup></b>	<b>cm</b>	
<b>CCRS</b>	0.75	20	-20
<b>LP</b>	0.60	25	-25

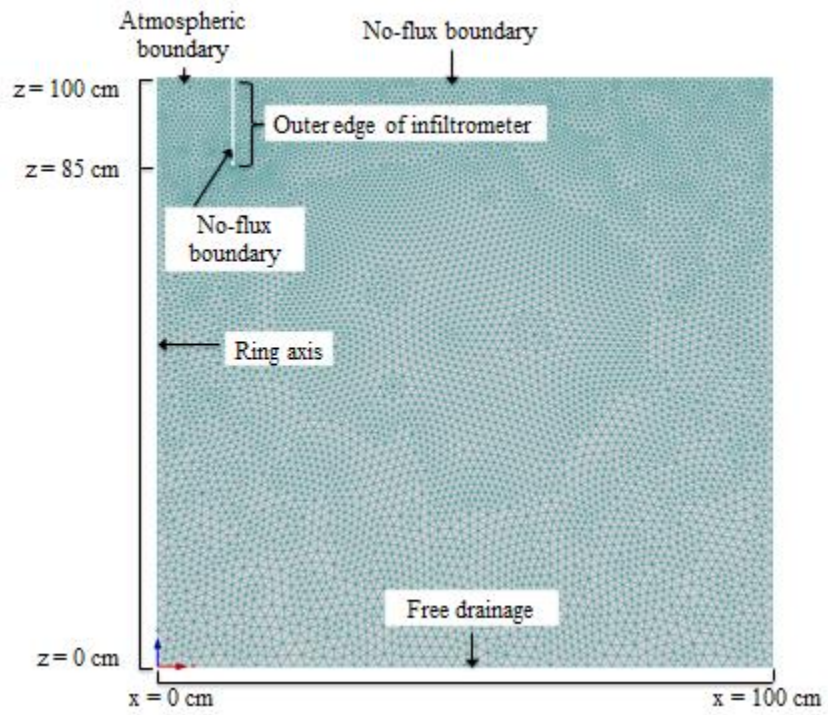


**Figure 3.1.** HYDRUS 2D domain geometry and boundary condition information for ring infiltrometer simulations.

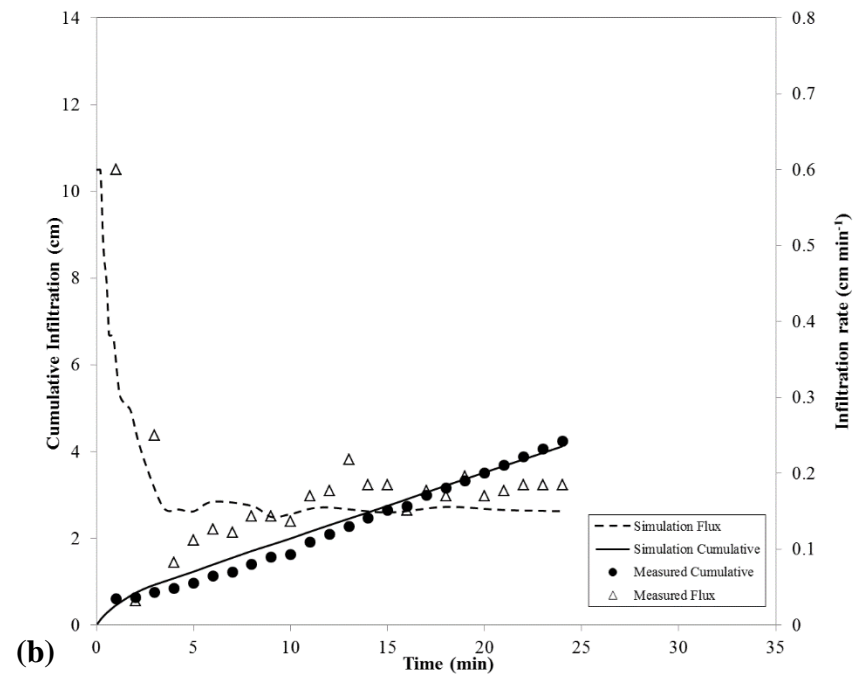
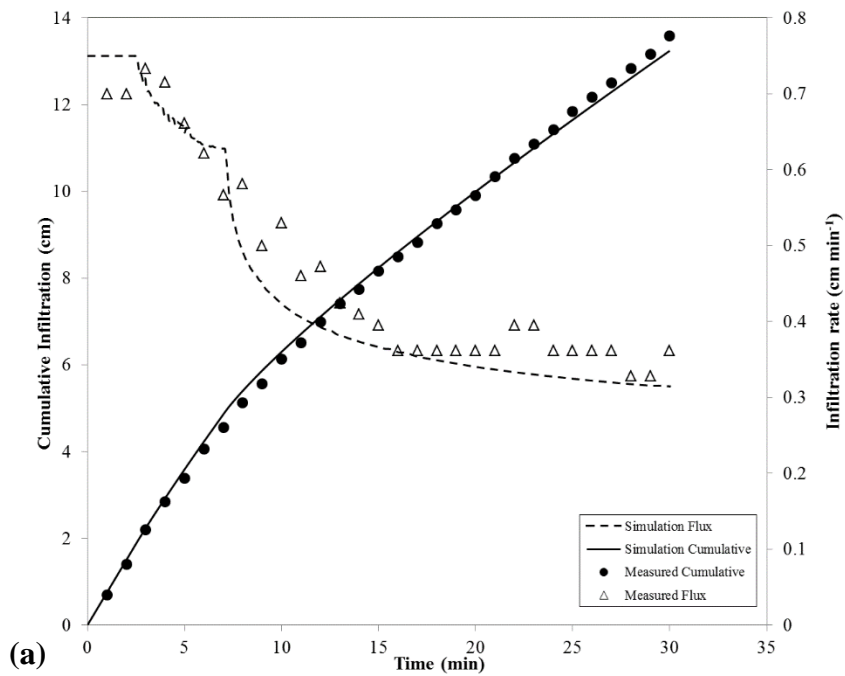


**Figure 3.2.** Simulation validation curves for CCRS (a) and LP (b) infiltrometer measurements.

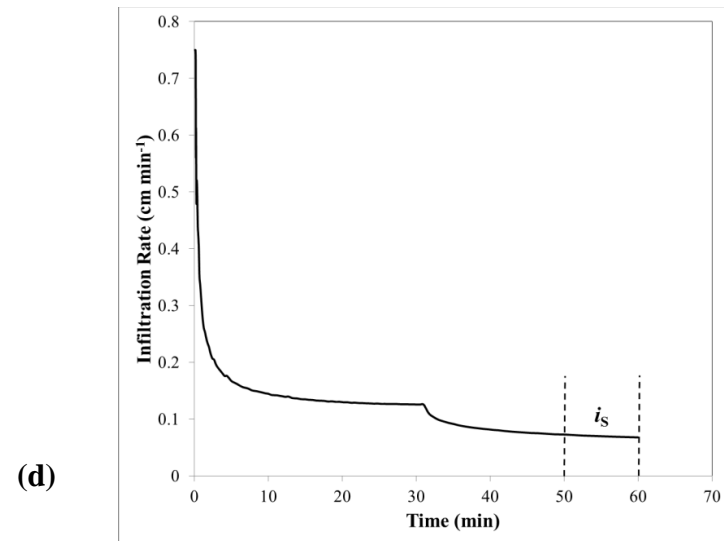
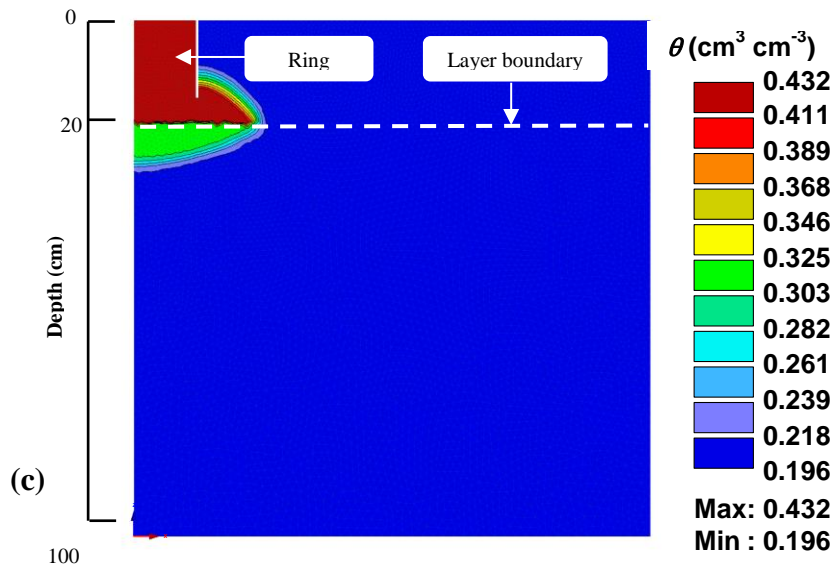
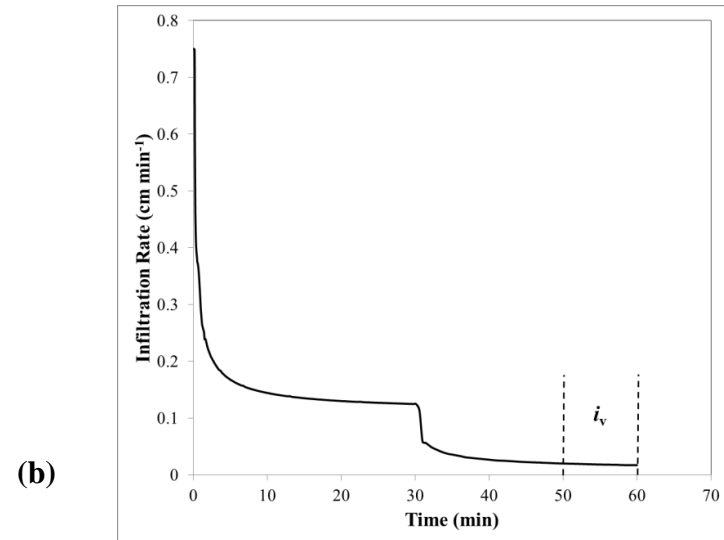
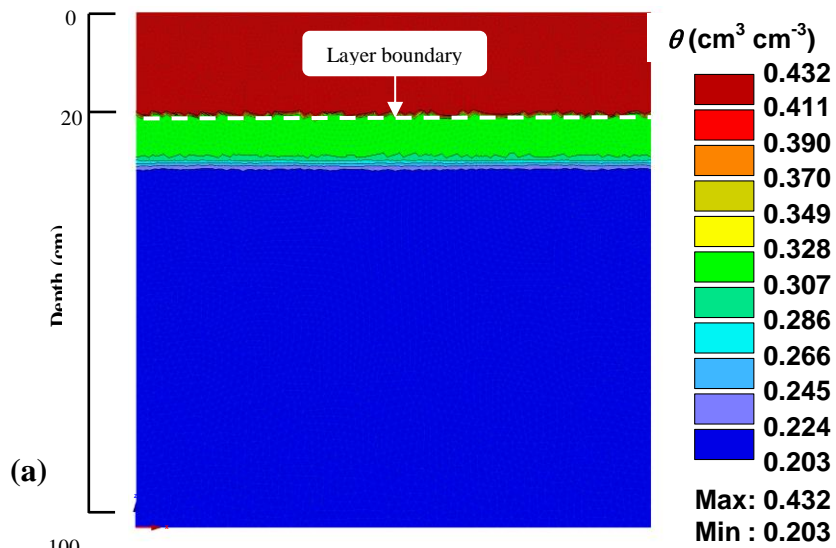


**Figure 3.3.** Example vertical infiltration rate ( $i_v$ ) water content distribution (a) with infiltration rate curve (b) and example CSI steady infiltration rate ( $i_s$ ) water content distribution (c) with infiltration rate curve (d) for 60 min. simulation using CCRS conditions.

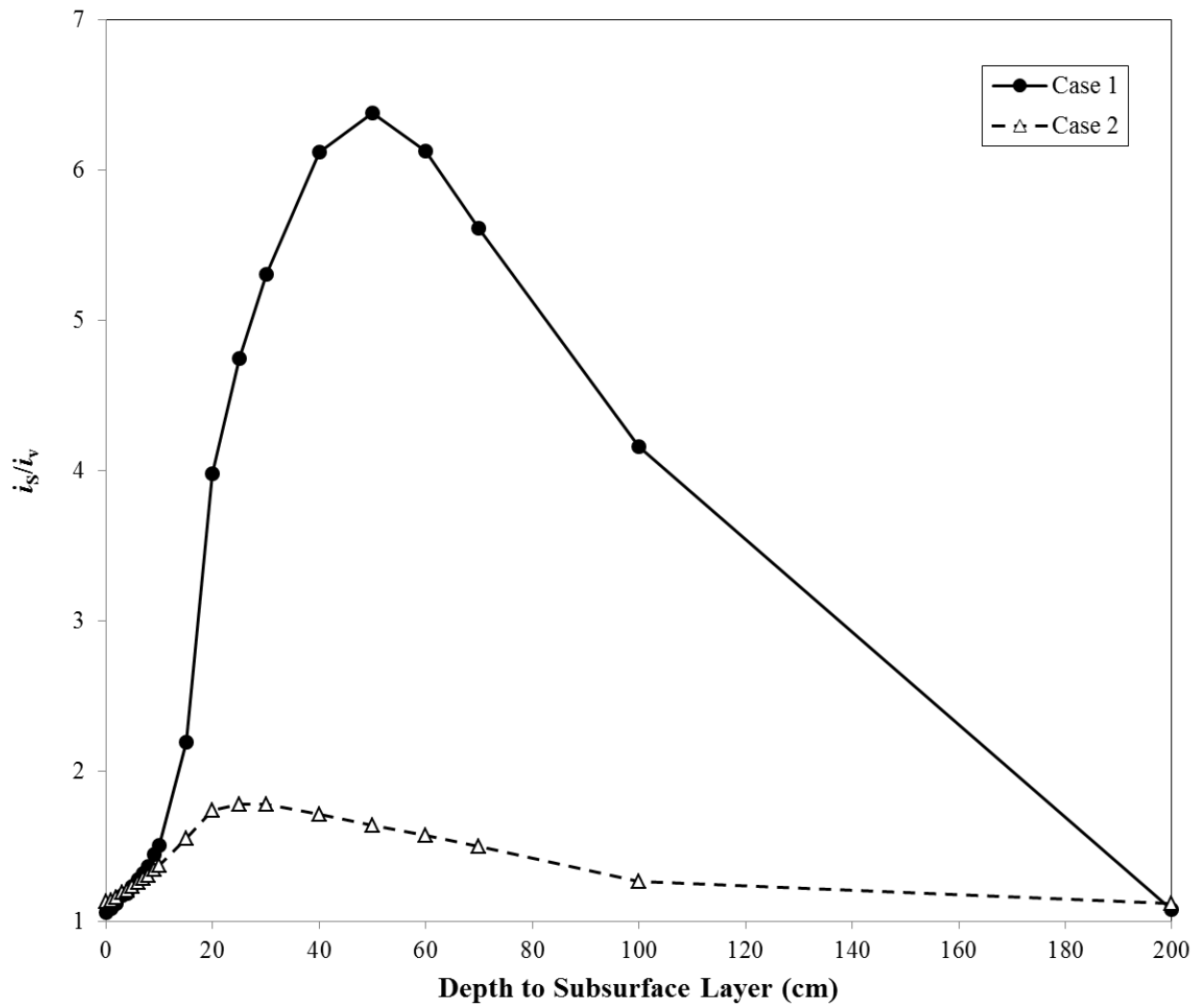


**Figure 3.4.** Numerical simulation results showing effect of layer depth ( $L$ ) on steady infiltration rate ( $i_s$ ) from the CSI method.



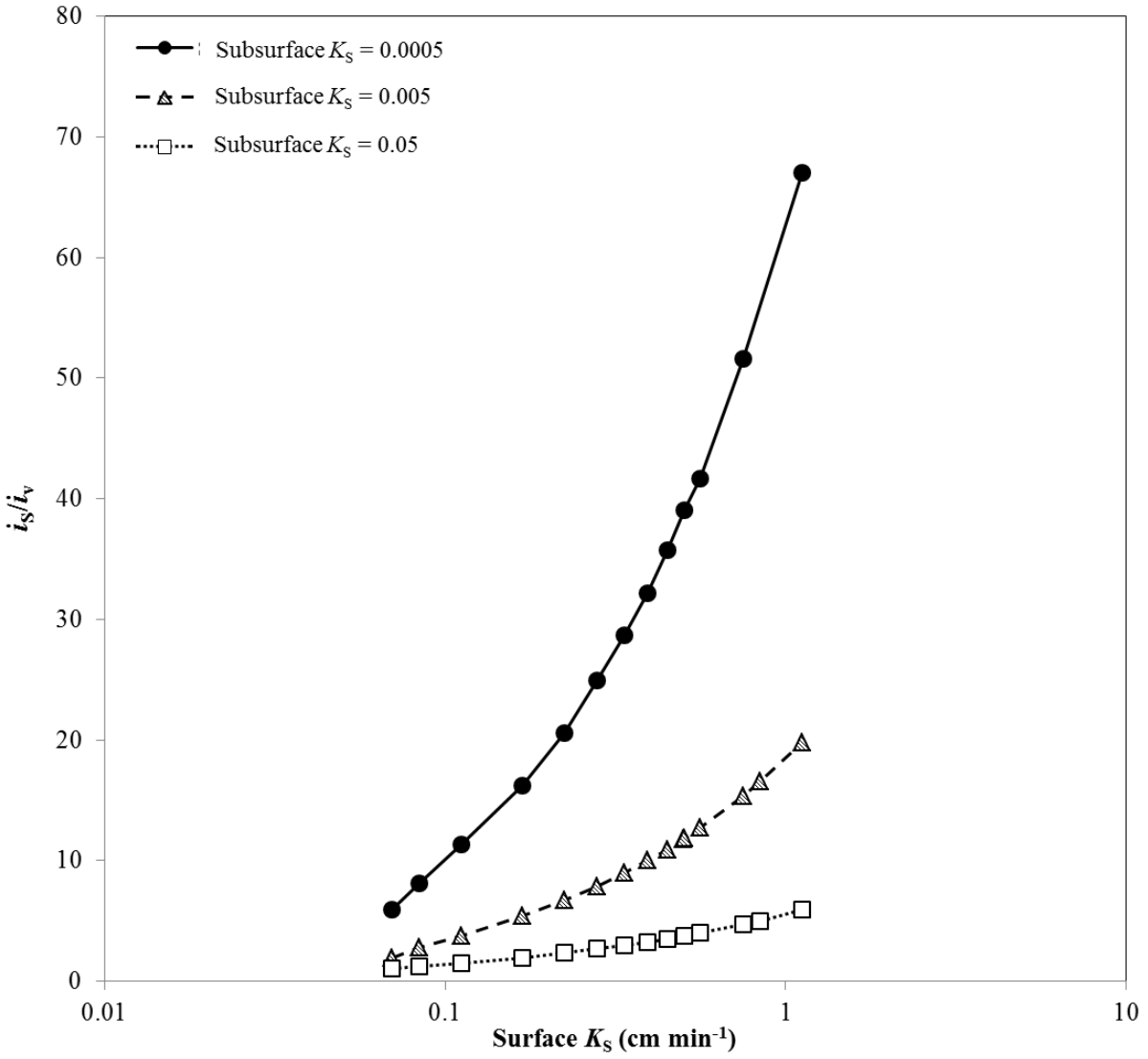


**Figure 3.5.** Numerical simulation results showing effect of layer  $K_s$  on steady infiltration rate ( $i_s$ ) measured using the CSI method for CCRS conditions.

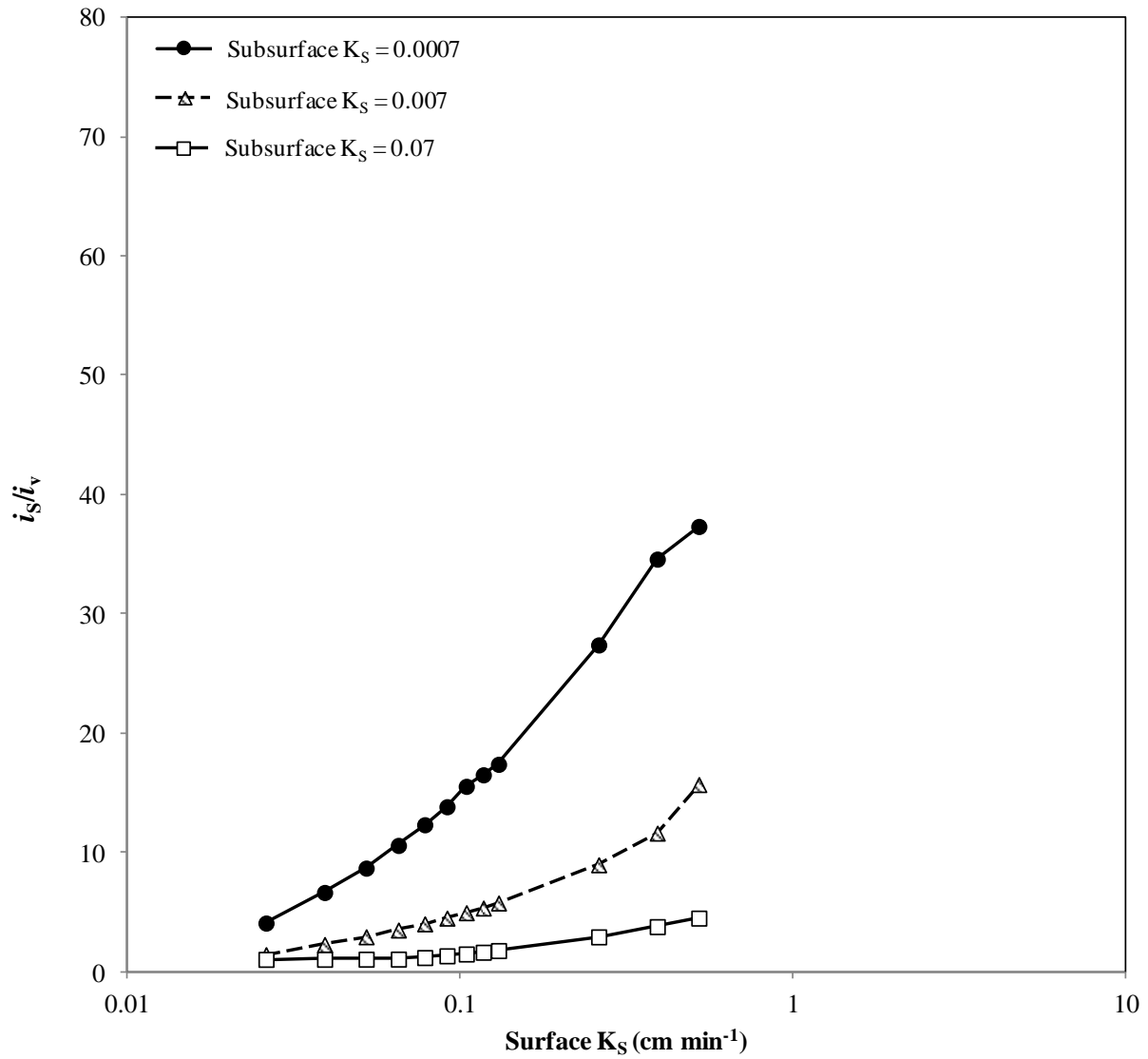


**Figure 3.6.** Numerical simulation results showing effect of layer  $K_S$  on steady infiltration rate ( $i_s$ ) measured using the CSI method for LP conditions.

## Chapter 4: Conclusions and Future Work

### CONCLUSIONS

The research presented was motivated by a need to assess the Cornell Sprinkle Infiltrometer (CSI) method for evaluating management practices designed to improve stormwater infiltration into soils. This assessment was carried out by conducting a comparison with a more commonly-used method using field experiments and by performing numerical tests based on soil properties. Two secondary objectives were established during the course of this research: 1) to determine the influence of soil layering effects created by management practices on infiltration measurements; 2) to relate infiltration rate measured using ring infiltrometers ( $i_s$ ) to one-dimensional vertical infiltration rate ( $i_v$ ) representing conditions consistent with rainfall infiltration into layered soils.

A comparison of  $i_s$  between the CSI method and the ASTM standard double-ring infiltrometer method (DRI) is presented in Chapter 2. Measurements from both methods were conducted on managed soils displaying a range of layered physical and hydraulic property conditions. Results indicate that  $i_s$  was comparable for both methods (2% greater overall for the CSI) and that correlation between methods was strong ( $R^2 = 0.79$ ). An attempt to relate  $i_s$  to soil properties was made in order to address the secondary research objectives. The  $i_s$  was hypothesized to be related to the subsurface layer saturated hydraulic conductivity ( $K_s$ ). A linear regression between  $i_s$  and subsurface layer  $K_s$  had strong correlation for both methods ( $R^2 = 0.87$  and  $R^2 = 0.83$  for single- and DRI methods, respectively), but data were distinctly clustered based on depth to subsurface layer. Further development of this equation may allow for more direct interpretations of ring infiltrometer measurements used to evaluate practices that create layered soil conditions.

CSI infiltrometer measurements were tested numerically for various layered soil conditions in Chapter 3. Experimentally validated simulations were used to determine effects from soil layering on the relationship between  $i_S$  (subject to lateral flow) and  $i_v$  (controlled by subsurface  $K_S$ ) for two case studies. The layering effects tested included  $L$  and layer  $K_S$  contrast. Depth effect tests where  $L$  was incrementally increased showed that  $i_S$  relative to  $i_v$  ( $i_S/i_v$ ) reached a depth-dependent maximum intrinsic to contrast in layer  $K_S$ . The results presented in Chapter 3 provide an indication of the degree to which lateral flow from CSI's may exaggerate measured values. Only extreme cases where layer  $K_S$  contrast was greater than one order magnitude did the results have substantial  $i_S/i_v$ . When layer  $K_S$  contrast was one order of magnitude or less,  $i_S/i_v$  was small, indicating that  $i_S$  gives values similar to  $i_v$ . Overall, the results indicate that the CSI method allows for adequate interpretations of  $i_v$  for layered soil conditions.

## **FUTURE WORK**

The research presented satisfied the method comparison question, but further investigation into the layered property effect is warranted. A general equation relating  $i_S$  to  $i_v$  that contains a term based on depth to subsurface layer and subsurface  $K_S$  may exist, though other factors are likely required. Terms including ring depth and surface layer  $K_S$  should be considered for future development of an expression relating  $i_S$  to  $i_v$ . The interaction between the measurement method constraints and layer properties should also be considered. It is likely that  $i_S$  may also be affected by the upper surface boundary condition (pressure head or rainfall rate) within the ring. Results from Chapter 2 show that  $i_S$  may be related to subsurface  $K_S$ , but that this relationship may be affected by depth to the subsurface layer. The effect of the upper boundary condition was not considered for the numerical simulations in Chapter 3, and inclusion of this factor may have provided insight into the determination of a general relationship for  $i_S$  and

$i_v$  for various layered conditions. The initial objectives of this study were to compare the two infiltrometer methods and to determine a range of expected results from various soil conditions using numerical simulations. A specifically-targeted investigation of infiltrometer measurement interpretations in management-induced layered soil conditions with regard to the upper boundary conditions may prove insightful for directly relating these measurements to natural rainfall events.